Torres-Lopez J, Tao L, Xiao L, Hu Z.

Experimental study on the hydrodynamic behaviour of an FPSO in a deepwater region of the Gulf of Mexico.

***Ocean Engineering* 2017, 129, 549-566**

Experimental Study on the Hydrodynamic Behaviour of an FPSO in a Deepwater Region of the Gulf of Mexico

Jaime Torres Lopez[1,3], Longbin Tao[1*], Longfei Xiao[2], Zhiqiang Hu[2]

1. School of Marine Science and Technology, Newcastle University, Newcastle upon Tyne, NE1 7RU, UK
2. Shanghai Jiao Tong University, Shanghai, 200240, China
3. Pemex, Exploration & Production, PEP, Marina Nacional 329 C, 11300, Cd. Mexico, Mexico

ABSTRACT

As offshore oil and gas exploration moves progressively toward greater water depths, it becomes more challenging to predict the environmental forces and global responses of floating production storage and offloading (FPSO) systems and the dynamic behaviour of the mooring lines and risers. The validation of complex numerical models through scale model experimental testing is restricted by the physical limits of the test facilities. It is not feasible to install the equivalent full length mooring lines and riser systems and select an appropriate scale model for reducing the uncertainties in the experimental test programme for deepwater and ultra-deepwater conditions. The combination of an appropriate scale FPSO model with a suitable level of equivalent effect reduced depth using a hybrid passive truncated experimental methodology for the mooring lines and risers is a practical approach.

Following recent discoveries, FPSO has been proposed for a portion of the planned development in the southern Gulf of Mexico (GOM) in water depth ranging from 1000 to 2000 metres. Based on a scale model and a hybrid passive truncated experimental method for mooring lines and risers, this paper investigates the global response of an FPSO, as well as the dynamics of mooring lines and risers in the context of prevailing environmental conditions for field development in a specific deepwater location in GOM. The experiments revealed that the main horizontal motion response of the FPSO (surge) under non-collinear loading condition is almost two-times that of the collinear loading condition. The mooring lines in the non-collinear condition are more sensitive to the dynamic response and risers appear to have an important influence on the low frequency damping.

Key Words:

Hydrodynamics, FPSO, Mooring lines, Non-collinear, Deep-water

1. Introduction

Scaled model tests of a ship-shaped FPSO, complete with turret mooring lines and risers in deepwater or ultra-deepwater locations, are considered to be the most reliable way to study the complex hydrodynamics and aerodynamics of the complete system (BMT, 2000; Stansberg et al., 2002). Using facilities fitted with advanced equipment, dedicated model tests can closely represent the motion response to realistic environmental conditions and dynamic interactions between waves, current, winds and the total floating system, including mooring and riser systems.

The experimental tests help to provide crucial information about the complex linear and nonlinear hydrodynamic behaviour of the total system, such as the total viscous damping contributions of the system, the coupled effects of the FPSO vessel with the mooring lines and risers, and the transient green water and slamming forces and wave run-up effects that are difficult to evaluate through numerical simulation alone, without any simplifying assumptions (Faltinsen, 1990; Chakrabarti, 1998; Luo et al., 2004). Thus, a model test is often used to validate designs throughout a complex iterative design process, typically using numerical tools.

However, when conducting model tests of offshore structures for deepwater and ultra-deepwater installations, scale effects become a major issue, and they are very difficult to handle due to the limited physical dimensions of the offshore basins (Stansberg et al., 2002; Chakrabarti, 2005). To limit the scale effect, a scale ratio of 1:50-1:70 has been recommended for model tests of FPSO systems and has been found to be reliable for predicting the full-scale behaviour (ITTC07-3.5, 2008). However, this range of scale ratios is unable to represent a full-

scale water depth when it is equal or greater than 1000 m, and the experiments involve testing the mooring arrangement and riser system behaviour (ITTC07-3.5, 2008).

Continued efforts have been made to overcome the test basin limitations by using relatively small models. A scale ratio of 1:170 is considered to be close to the practical limit, particularly for examining the hull behaviour, based on existing model basin facilities and limitations (Moxnes, 1998). Small-scale testing of 1:150-1:170 has been undertaken, and studies on reliability at this scale have been suggested to evaluate and quantify the uncertainties and to keep them within acceptable levels of accuracy (Stansberg et al., 2004). An alternative procedure, called the hybrid passive methodology, has been explored. It combines an appropriate scale model for the FPSO hull with a depth truncation to yield an equivalent effect of mooring lines and risers in responding to the test basin limitations. Such an effect represents the appropriate forces from mooring lines and risers on the motions of the vessel, which are computed with a numerical simulation procedure by extrapolation to the motion responses of the design prototype system in full water depth (Chakrabarti, 1998; Tahar, 2003; Luo et al., 2004; Fylling, 2005; Baarholm *et al.*, 2006; ITTC07-3.5, 2008; Su *et al.*, 2009).

Stansberg et al. (2000) investigated this approach and made a comparison for a moderate water depth using both the hybrid passive methodology and a full depth model with a conventional scale model. The results showed that the truncated mooring and riser model approach is technically feasible.

On the other hand, the collinear and non-collinear environmental condition of waves, wind and current often occur in deepwater regions of the GOM. Baar et al. (2000) observed that the extreme response of a turret-moored FPSO is sensitive to the non-collinear environmental conditions of waves, current and wind and the location of the internal turret has influence on the motion response and tension of the mooring lines. Irani et al. (2001) and Ward et al. (2001) showed that the response of moored FPSO is more severe in non-collinear environmental

conditions, but non-collinear conditions have less influence on the tensions of the mooring lines.

This paper describes an experimental study on the dynamics of a complete FPSO-mooring-riser system in a deepwater location using the hybrid passive truncated experimental method for the behaviour of the lines and risers. The experimental test was undertaken in an offshore basin with 10 m of water depth, and the main focus was to study the nonlinear hydrodynamic effects on the FPSO vessel coupled with both mooring lines and risers. The FPSO global responses for both the full and the ballast loading conditions and the associated dynamics of the mooring lines and risers were studied for collinear and non-collinear environmental conditions.

2. Model system description

The FPSO used in the study is 300 m in length between perpendiculars with a breadth of 46.20 m and a depth at the side of 26.20 m in prototype dimensions. The hull has a simple form, and the middle cross section of the model is box-shaped (see Fig. 1a and Fig. 1b).

Both the Full load and Ballast load conditions were tested. The Full load condition is associated with a level keel draught equal to 16.5 m with a corresponding displacement of 218,876 tonnes, and in the Ballast load condition, the average draught was 9 m with a corresponding displacement of 122,530 tonnes. The total mass in the scale model was achievement in less than 1 % between the measured and target total (measured values: 216,800 tonnes and 121,400 tonnes) for Full Load condition and Ballast load condition respectively.

A crude topside arrangement was used with a beam area on the deck of 5190 m^2, and a bow area on the deck 1448 m^2, sufficient to allow evaluation of the wind loading on a typical topside area on the FPSO model. The hull of the FPSO included a bilge keel of 1.00 m width and 120 m length.

106 The FPSO model was fitted with an internal turret mooring lines system, which has a
107 diameter of 12 m in the prototype. Its vertical centre line was located 30 m aft of the forward
108 perpendicular of the FPSO vessel. The function of the turret was to provide a tie-in mechanism
109 for the FPSO, with 9 mooring lines and 6 risers enabling the hull to yaw relative to the mooring
110 lines and risers. In the experimental test, the Froude and Strouhal number of the model and
111 prototype were kept the same making the gravitational and inertial forces similar. The main
112 particulars of the FPSO vessel in the prototype and the corresponding model scale dimensions
113 are summarized in Table 1.

114 A permanent mooring line system was designed to allow for the expected extreme motion
115 values of the FPSO vessel and the maximum tensions of the lines. The mooring system was
116 reviewed for both intact and assumed single line damage conditions using both collinear and
117 non-collinear combinations of environment loading cases of one significant event of storm and
118 hurricane conditions for a 100-year return period (API-RP-2SK, 2005). The mooring line
119 system has 9 lines with a symmetric configuration arranged in three groups, each group having
120 3 lines. The groups were 120 degrees apart, as shown in Fig. 2, Case B. The individual lines
121 are identical, and each one has three integrated chain-spiral and strand-chain segments. Each
122 line in a group is separated by 5 degrees from the adjacent line. The mooring system was
123 established, and each line was semi-taut but had a simple catenary mechanism that was
124 subsequently verified through the slightly non-linear behaviour of the restoring force curves
125 and offset as shown in Fig. 3. Comprehensive details and characteristics of the mooring lines
126 are given in Table 2.

127 Six steel catenary risers (SCR) for production and potential injection were assumed with a
128 simple symmetric configuration. The risers were selected only for including and evaluating
129 their typical static and coupled associated dynamic effects on the vessel. The riser
130 arrangement in three groups is shown in Fig. 2, Case C, in which each the groups are all
131 separated by 120 degrees. The main riser characteristics are given in Table 3. Considering
132 the offshore basin dimensions and the instrumentation capacity for environments and
133 measurements, a model scale of 1:64 was chosen for the experiments to minimize the scaling

effect. A passive hybrid method was used to design the truncated mooring lines and risers with an equivalent effect to represent installation at 1000 m. The complete FPSO with truncated mooring and riser system was tested in the Deepwater Offshore Basin at Shanghai Jiao Tong University (SJTU).

Both the mooring lines and risers were thus truncated to 627 m depth in the full-scale. The choice of the model scale and level of truncation were thus selected to minimize the uncertainties related to scaling effects on all system components. The criteria for the design of the truncated mooring system seek to model as closely as possible the following parameters of the full prototype system:

- Total horizontal stiffness-offset of the system
- Representative single line and riser tensions
- The number of components and layout of mooring lines and risers

A static analysis was performed to design a system of truncated mooring lines and risers that satisfies the horizontal restoring forces characteristics of the full depth prototype system for the three principal horizontal directions (180 degrees, 90 degrees, 0 degrees). A procedure similar to that presented by Waals et al. (2004) and the ITTC (2008) was used to evaluate the design of the truncated mooring line and riser system.

The comparison of the restoring forces of the full depth prototype system and truncation design for the mooring lines and risers is shown in Fig. 3a. Additionally, the top tensions of the most loaded mooring lines and risers of each group is shown in Fig. 3b.

Maximum differences of approximately 8% were observed in the general restoring forces between the truncated and the prototype design in the horizontal aft direction of 0 degrees, which were considered acceptable. In the other directions, 180 degrees and 90 degrees, smaller differences were observed. A similar discrepancy was observed for the most critical line tension and riser tension, demonstrating that good agreement was achieved between the truncated system model and the full depth model. The maximum horizontal spread length at model scale was 15.48 m for the mooring lines and 13.79 m for the risers, which could fit within

the length and width of the measuring area of the basin. The main characteristics of the prototype and the corresponding truncated mooring line and riser systems are shown in the Table 2 and Table 3, respectively.

The truncated mooring line system was built using combined chain and spring segments to provide the appropriate submerged weight, axial stiffness (EA), pre-tension and restoring force contributions for each of the mooring lines (Fig. 4).

For the model tests, the six risers were also built of wire and spring segments to satisfy the main requirements of the truncation design, such as the submerged weight, EA, pre-tension, and restoring force characteristics. The bending moment capabilities of the riser section were not taken into account in the design (Fig. 5).

3. Experimental setup

a. Model setup

The experimental model test was performed in the Deepwater Offshore Basin at Shanghai Jiao Tong University (SJTU) in China. The dimensions of the basin are 50 m by 40 m, with a total available water depth of 10 m that can be adjusted through a vertically moveable bottom floor. The plan view of the basin is given in Fig. 6. The basin was fitted with environment simulation equipment, including a multi-flap wave generation system, a current generation system and a wind generation system capable of creating both collinear and non-collinear directional environment loading conditions. The six-degrees-of-freedom motion of the FPSO model were captured through an optical motion tracking system, in which four passive tracking targets were installed on the stern of the FPSO model vessel. The conversion of the tracking target positions to rigid body motions at desired reference point is achieved through proprietary software licensed by Qualisys (2010).

The tensions in the mooring lines and risers were measured using fifteen sensors installed individually at the fairlead connection points of each lines and risers.

b. Loading conditions

Both collinear and non-collinear environmental conditions are often observed in the specific location of the GOM. For this study, the cases included both situations, which are defined for the storm conditions of a 100 year return period. Fig. 7 shows the three cases of collinear (2 cases) and non-collinear conditions (1 case), with a wind direction of 60 degrees and current direction of 90 degrees of the waves. The irregular waves with current and wind governed the main part of the test programme, and the test duration for each case corresponded to three hours in the prototype.

c. Testing matrix

The experimental test programme consists of the following main components:

- Calm water decay tests in the 6 DOF of the freely floating FPSO model for Full and Ballast load conditions
- Calm water decay tests of the floating FPSO model with mooring lines only, and with mooring lines and risers for Full and Ballast load conditions
- Horizontal stiffness (restoring forces) of the mooring lines and risers
- White noise wave tests (head, beam and quartering direction)
- FPSO model motions in six DOF at the turret and tension force components at the turret fairleads for the 9 mooring lines and 6 risers
    - Collinear 'In-lines' mooring lines loading condition of irregular waves only
    - Collinear 'In-line' and 'Between-lines' mooring lines loading conditions of the simulated irregular waves, current and wind for Full load conditions
    - Non-collinear combinations of environment loading condition of irregular waves, current and wind for Full and Ballast load conditions

Three configurations were considered as the basis to study the hydrodynamic behaviour of the FPSO itself and a complete system of the FPSO with mooring lines and risers. The arrangement for "Case A" only considered the FPSO model with temporary horizontal

restraining lines fitted above of the water. “Case B” was for the FPSO model with mooring lines only, and the arrangement for “Case C” was the FPSO model, together with full mooring lines and risers (see Figure 2).

d. Static characteristics of the mooring line and riser systems

The static characteristics of the mooring line and riser systems obtained from the experiment and the numerical design were verified. The longitudinal directions (180 degrees and 0 degrees) corresponding to ‘In-line’, and ‘Between-lines’ conditions, and transverse direction (90 degrees) displacements corresponding to surge and sway were compared. Figs. 8 and 9 show a very good agreement of restoring characteristics (maximum offsets) in the alternative fore and aft longitudinal directions (180 degrees and 0 degrees) with mooring lines with and without the risers. Furthermore, the tensions for the most highly loaded mooring line and riser were also examined, and the tension levels obtained in the experiment and the numerical design for the surge direction (180 degrees) showed good agreement.

Fig. 10 shows a comparison of the restoring forces of the sway in the transverse direction (90 degrees) between numerical results for the truncated mooring and riser system and those measured in experiment. It is seen that the truncated numerical results agree well with the experimental measurements up to 60 m offset and the difference slightly increases afterward. As it is expected that there will be a mean dynamic response of 30 to 50 m in this direction, thus, the similarities of the restoring characteristics were considered to be reasonable in sway. Furthermore, the contribution of restoring forces from the risers in this direction was found to be negligible.

4. Metocean conditions

A storm condition for a 100-year return period was selected to study the hull motion responses and the associated dynamics of the mooring lines and risers. The JONSWAP spectrum was chosen, with the characteristics of a significant wave height of 9.67 m and a peak wave period of 13.28 s. The wind velocity at 10 m reference height for one hour was 21.95 m/s. The current velocity on the surface was 1.44 m/s (see Table 4).

a. White noise wave calibration

A generated white noise wave environment was used to represent the full-size and full range environment with wave periods from 5 to 25 s and a significant wave height range of 0-3.25 m. This covered the range of incident wave frequencies for the operational Full load and Ballast load conditions of the FPSO model. Then, the white noise wave generation was calibrated with the specific parameters in the deepwater basin with the FPSO model used in "Case A" (Fig. 2). Fig. 11 shows very good agreement for the spectrum of the wave target and the measurements.

The generated white noise wave spectrum was subsequently used for the calculation of the RAOs in the head, beam and quartering sea conditions through a post-process analysis. For these tests, the FPSO model was held in the required position in the basin with the simple elastic restraining horizontal lines above water surface and set up in the wave heading directions of the studies.

b. Irregular wave calibration

The irregular waves in the basin were calibrated in the directions of 180 and 90 degrees. The characteristics were based on the significant wave height, the mean period, gamma shape factor for the JONSWAP wave spectrum (Table 4). These characteristics were selected to represent the typical environment of the southern region of the Gulf of Mexico.

Figs. 12 and 13 compare the generated irregular wave spectrum for the measured and the target waves in the 180 and 90 degree directions, respectively, showing that excellent agreement was achieved. The calibrated irregular waves in two different directions were used in conjunction with the current and wind generated to create the collinear and non-collinear environment loading conditions in the two directions during the experiment.

c. Wind load and current speed calibration

The mean wind load was only considered in the model test. The wind load was calibrated according to the total wind force calculated for Full Load (F_{full} = 428.68 kN) and Ballast Load

conditions ($F_{ballast}$ = 531.25 kN) for the FPSO in bow condition. In the case of the current velocity a point located near to the bow of the FPSO model was used to measuring and calibrated the surface current speed. The mean value and standard deviation of the measured current velocity were 1.43 m/s and 0.137 m/s respectively which made reasonable agreement with the target current velocity (1.44 m/s). Fig. 14 shows that the current fluctuations tend to increase significantly in frequencies smaller than 0.023 rad/s and thus a slight influence on the slow-drift motions is expected.

5. Results and discussion

This section presents the results and analysis of the experimental measurements, and it is organized in the following sub-sections: Decay tests, RAOs from white noise wave tests, spectrum analysis and statistical analysis of the FPSO motion response and the dynamics of the mooring lines.

a. Decay tests

-FPSO model only

Decay tests were carried out in calm water for the six DOF of the assumed uncoupled motions of the FPSO model for Full load and Ballast load conditions. The test arrangement Case A shown in Fig. 2 with temporally horizontal restraining lines above of the water was used. Based on the decay tests of the FPSO model in calm water, the natural periods and one average value of the damping ratios of the FPSO hull based on the logarithmic decrement method were calculated (Chakrabarti, 1994).

The first cycle of measurement for each decay test were discarded to allow a short period of time for attenuation of any transient loads that may have been induced, and the time series of the signals were then recorded for the decay tests.

Table 5 shows that the natural periods of the FPSO model in the Full load condition were in general higher than those in the Ballast Load condition. This shows a strong influence of the

model displacement and the hydrodynamic restoring force characteristics on the natural periods.

The relationship between the logarithmic decrement and the peak amplitudes and the local damping ratios for two adjacent cycles can also be evaluated by the relation: (Journee et al., 2001):

$$\zeta = \frac{1}{2\pi} \ln\left\{\frac{y_n}{y_{n+1}}\right\} \quad \text{vs} \quad \bar{y} = \frac{y_n + y_{n+1}}{2} \tag{1}$$

Where:

ζ = Local damping ratio (ratio between damping and critical damping)

y_n and y_{n+1} = Two succeeding amplitudes at a time interval of period of oscillations

Then the damping ratios can be shown from two successive positive peak amplitudes.

The damping ratios in surge for both the Full and Ballast load conditions showed similar linear trends. Fig. 15 shows the variation for the surge damping ratios from two successive positive peak amplitudes for the Full load condition (from 0.011 to 0.017), which was slightly higher than that for the Ballast Load condition (from 0.011 to 0.014). The submerged surface area of the hull of the FPSO model appeared to have a slightly greater influence on the viscous damping contribution, whereas the dependency on the mean surge amplitude appears to be negligible, indicating that flow separation does not occur in this case under the Reynolds number at model scale. Additionally, skin friction is dominant in the viscous damping for surge motion.

-FPSO model together with mooring lines in the Full load condition

Similarly, surge decay tests for the 'In-line' and 'Between-lines' conditions of the FPSO model with the truncated mooring lines for the Full Load condition were carried out. The test arrangement shown in Fig. 2 Case B was used for the decay test in calm water. The natural period for the 'In-line' case was found to be 353.57 s and 362.05 s for the 'Between-lines' case.

326 The slightly higher natural period for the 'Between-lines' case was due to a reduced
327 contribution of the horizontal restoring forces from the truncated mooring in this direction, as
328 shown in Figs. 8 to 9.

329 In contrast to case A (Fig. 2), the damping ratios obtained from the decay tests of case B
330 (Fig. 2) were dependent on the amplitude of oscillation, primarily due to the flow separation
331 from the interaction of the mooring lines with the calm water. Fig. 16 shows that the estimated
332 damping ratios are almost at the same level of magnitude for both collinear cases ('In-line' and
333 'between-lines').

334

335 *-FPSO model with both mooring lines and risers in the Full load condition*

336 The full arrangement of the FPSO model was also tested, together with the truncated
337 mooring lines and risers. The two different directional arrangements ('In-line' and 'Between-
338 lines') were also used to evaluate the additional effects of the riser system (see Fig. 2, case
339 C). The natural period for the 'In-line' case was found to be 339.35 s, and for the 'Between
340 lines' case, the natural period was found to be 344.18 s.

341 Fig. 16 shows the trends of the damping ratios of the FPSO model with mooring lines and
342 the FPSO model with mooring lines and risers, for the 'In-line' and 'Between-lines' cases in
343 surge direction, respectively. Significant contributions of the mooring lines and the risers to the
344 total damping of the complete system are evident. Notably, the riser system makes a greater
345 contribution to the overall damping for the 'In-line' case in the surge direction.

346 The natural period and the estimated average damping ratios of the 'In-line' and 'Between-
347 lines' cases are shown in Table 6.

348 *b. Motion response – linear transfer functions (RAOs)*

349 The RAOs for each of the six DOF were calculated at the C.G. of the FPSO model. The
350 directions of the white noise waves for the studies were, relative to the ship, head seas (180^0),
351 quartering seas (135^0) and beam seas (90^0) conditions.

352 *- FPSO motion in head seas*

353 The surge, heave and pitch motion RAOs of the FPSO model are the most important motion
354 modes for the head sea conditions (Fig. 17). Both the Full load and Ballast load conditions for
355 surge RAO show a slightly coupled effect, with the heave motion near the heave natural
356 frequency (ω=0.54 rad/s) and the maximum amplitude increasing at a lower frequency of 0.45
357 rad/s. Differences between the Full and Ballast load conditions were found to be insignificant.
358 On the other hand, slight differences between the Full and Ballast load conditions for the heave
359 RAO were observed near the natural heave frequency, which shows that the magnitude of the
360 heave RAO for Full load condition was slightly higher than that for the Ballast Load condition.
361 Furthermore, the amplitude of the pitch RAO close to the natural frequency, was relatively
362 small, which is attributed to the fact that the length of the FPSO model's is greater than the
363 incident wave length.

364 *- FPSO motion in beam seas*

365 For the beam seas incident wave condition, roll, sway and yaw RAOs are the most
366 important. For both Full and Ballast load conditions, Fig. 18 shows no significant differences
367 in the sway, pitch and yaw RAOs. However, the roll RAOs for the two load conditions show
368 differences in both amplitude and resonant frequency. The roll RAO for the Full load condition
369 possesses a higher maximum peak amplitude at a frequency equal to 0.47 rad/s than that for
370 the Ballast load condition. In contrast, the shape of the roll RAO for the Ballast Load condition
371 is wider than the roll RAO for the Full load condition.

372 *- FPSO motion in quartering seas*

373 Furthermore, for the quartering sea incident wave condition, the six DOF, surge, sway,
374 heave, roll, pitch and yaw motion RAOs are all important. All six DOF motions show coupled
375 effects for both Full load and Ballast load conditions (Fig. 19). The highest amplitude is
376 observed in the roll motion which is similar for Full and Ballast load conditions, whereas the
377 resonance frequency is smaller for the Full load (0.50 rad/s) compared to the Ballast load

condition (0.58 rad/s). Differences between the Full load and Ballast load conditions for the other motions were found to be insignificant.

The amplitude of motion responses of the RAOs are sensitive to the direction of the incident wave, and the differences between the Full and Ballast load conditions were found to be insignificant, except for the roll motion, which showed slight differences in resonant frequency responses and maximum peak motion amplitudes.

The motions responses of the RAOs from experimental and calculated numerical using a commercial computer program SESAM (2014) were compared for Full Load condition. The viscous roll damping was identified to be important to the roll RAO while those for surge, sway, yaw, pitch and heave appeared to be less important. This was attribute to that the roll motion RAO is dominated by the resonant response and which has the strong influence from the viscous effects due to the vortices that are generated by the bilge keels of the FPSO model, whereas the other linear motion RAOs are largely governed by the inertia of the FPSO model.

Figs. 20 to 25 show the RAOs for the six DOF in the Full Load condition. It is observed that the experimental results provide a good agreement compared to the numerical analysis. Thus the measured RAOs for the model FPSO reliably reproduced that of the prototype FPSO calculated numerical.

c. Motion response spectra for the FPSO

The motion response spectra in frequency domain of the six DOF were calculated using the time series from the experiments using the Fast Fourier transform. A by-pass filter equal to 4 for the low frequency range and 10 for the high frequency were applied to remove possible noise in the initial recorded signal.

i. FPSO in Collinear and non-collinear environments for the Full load condition

The motion response spectrum of the FPSO model, complete with the mooring lines and risers exposed to the collinear and non-collinear environmental load conditions of the irregular waves, current and wind were studied for the Full load condition, as illustrated in Fig. 7. The motion response spectra for surge, heave, roll and pitch were analysed. The surge motion response spectra of the FPSO model were analysed with mooring lines only, and with both mooring lines and risers.

-FPSO model with mooring lines only

The surge motion response spectra of the FPSO model in Full load condition for the 'Between-lines' and Non-collinear cases show the same level of maximum peak energy amplitude in the resonance frequency, whereas the 'In-line' case shows a smaller peak energy amplitude. This indicates that the 'In-line' case provides more damping from the mooring lines, while 'Between lines' case and Non-collinear case have less restoring force contribution in the surge direction with slightly lower resonance frequencies (Fig. 26). The motion response spectra show that only energy at the low frequency range has a notable influence on the global response, whereas the wave frequency response contribution is negligible in the surge direction. Furthermore, it is known that the wave-current interaction tends to influence the viscous drift damping that is responsible for the low-frequency surge motion (see, e.g., Dev 1996). As observed in Fig. 26, the peak of low-frequency surge response in collinear 'In-line' environment condition (wave+current+wind) is smaller than that in 'In-line' wave only condition, indicating that the wave-current interaction in collinear 'In-line' environment condition (wave+current+wind) increases the viscous drift damping on the FPSO model. On the contrary, the peak surge response in the non-collinear case (wave+current+wind) is larger than that in collinear environment condition (wave+current+wind), indicating that the wave-current-wind interaction in non-collinear environment condition decreases the viscous drift damping.

On the other hand, the wave frequency motions (roll, heave and pitch) were analysed for the collinear cases and the non-collinear cases and the results were presented in Figs. 27 to 29. Roll motion response for the non-collinear case was observed to have the highest energy amplitude (Fig. 27). The heave and pitch motion responses were also higher in the non-collinear case compared to the collinear cases (Figs. 28 to 29). The coupled heave and pitch motion responses were observed in both the collinear and non-collinear cases partly due to the resonance frequencies for pitch and heave are close to each other. Moreover, the origin of the body-fixed coordinate systems at which the surge, sway and heave motions are referenced is the turret location, which is near the bow of the ship. Consequently, the coupled geometric response between heave and pitch motions in which pitch motions tend to show up as heave in addition to pure vertical motions of the FPSO model. As can be seen in Figs. 28 and 29, the geometric coupling between heave and pitch is dominant effect than that due to energy transfer between the heave and pitch modes in this case."

For the most loaded mooring line, Fig. 30 shows that the highest peak energy amplitude of the line tension response spectrum is observed in the 'In-line' case (L-1) for the Full load condition, which is associated with the higher mean load condition compared to the other cases. The line tension response spectrum (L-1) shows that only the low frequency range energy has a dominant influence on the global response, whereas the wave frequency response contribution is negligible.

-FPSO model with mooring lines and risers.

The motion response spectra of the FPSO model with mooring lines and risers for the Full load condition were analysed for the environment loading case with the maximum motion responses identified previously (surge and roll motion in non-collinear cases). Fig. 31 shows the surge motion response with a peak energy associated with a low frequency of 0.018 rad/s, which was observed for the system with mooring lines only, and a frequency of 0.022 rad/s was observed for the system with both mooring lines and risers, respectively. The peak energy

455 at the resonant frequency of the FPSO model with mooring lines and risers decreases by
456 approximately 30% compared to the system with mooring lines only, due to the additional
457 damping contribution from the risers.

458 In the range of the wave frequency motion, the roll motion spectrum was analysed to
459 examine the influence of the risers on the roll motion response. Fig. 32 shows that the peak
460 amplitude decreases by 31% when the risers are included. However, the frequency associated
461 with the peak amplitude appears to be not affected by the risers, due to small contribution of
462 restoring forces from the risers. Fig. 33 shows the mooring line tension response for the
463 maximum loaded line (L-1) in the 'In-line' case, under the Full load condition. The response
464 spectrum for the maximum loaded riser (R-1) is presented in the non-collinear case (Fig. 34)
465 because the wave frequency motion response is slightly higher than the collinear cases.

466 *ii. Full vs. Ballast load condition for the non-collinear environment loading case*

467 The Ballast Load condition of the FPSO model in the test matrix was only considered in the
468 non-collinear case. A comparison between Full load and Ballast load conditions for the non-
469 collinear case was carried out for the maximum low frequency motion (surge motion) and
470 tension in the most critical mooring line.

471 Fig. 35 shows that the Full load condition has a higher peak amplitude compared with the
472 Ballast Load condition. Moreover, the influence of riser damping in the response amplitude is
473 important. The highest peak energy amplitude of the line tension response spectrum is
474 perceived in the FPSO model with mooring lines only, for the non-collinear case in the Full
475 load condition (Fig. 36).

476 *d. Statistical Analyses*

477 The time series motion responses in the six DOF of the FPSO model in Full load and Ballast
478 Load conditions and the most loaded mooring line and riser were further examined. The
479 collinear 'In-line', 'Between-line' and Non-collinear environment conditions of the irregular

480 waves, current and wind, as previously defined, were used in the analysis. The comparisons
481 were made in terms of their statistical properties such as the mean, minimum and maximum
482 values and the associated standard deviations in full-scale.

483 The detailed experimental information of the time series yaw motion responses and offset
484 trajectories along of turret centre for the non-collinear case can be seen in Figs. 37 to 44.

485 *i. Collinear vs. non-collinear environment loading cases for the Full load condition*

486 *-FPSO model with mooring lines*

487 The maximum motion responses were observed to be in the low frequency range in the
488 surge direction for all environmental loading cases. The maximum motions occurred in the
489 surge direction due to the mooring line/internal turret system, which allowed the FPSO to rotate
490 freely about the moorings, similar to a weather vane and to point in the direction of least
491 resistance against the various combined components in the environment loading conditions.

492 A maximum surge motion response of -86.62 m occurred in the non-collinear case for the
493 arrangement of the FPSO model and mooring lines compared to the corresponding collinear
494 'In-line' condition (-56.93 m) and collinear 'Between lines' condition (-84.46 m) respectively, as
495 shown in Table 7. Clearly, negative values of surge motion indicate that the vessel is moving
496 in an aftward direction, the reciprocal to the conventional surge sense, as a result of the
497 weather vane rotation about the turret.

498 This behaviour is mainly due to the non-collinear environment loading condition, with the
499 current at 90 degrees relative to the incident wave, which increases the energy of the incident
500 irregular waves (Chakrabarti, 2005). Therefore, the mean and dynamic surge motion
501 responses increase in the FPSO model (Faltinsen 1994, Stansberg *et al.* 2013) owing to the
502 increase of the mean and slow-drift excitation wave. Based on the comparison was made
503 between collinear and non-collinear environmental loading conditions, the mean motion
504 response in the surge direction was observed to be higher in the non-collinear case (-43.24

m) compared with the collinear cases ('In-line' case = -28.86 m, and 'Between-lines' case = -35.67 m). The low frequency sway and yaw motions in the non-collinear case, in terms of absolute values, resulted in maximum motions of 34.18 m and 54.53 degrees, respectively, compared with the 'In-line' condition (sway=14.88 m and yaw=17.58 degrees) and the 'Between-lines' condition (sway=18.11 m and yaw=15.03 degrees).

On the other hand, the effects of the yaw motion in the wave frequency also influenced the motions of roll, heave and pitch. In the non-collinear case, the motions in terms of absolute values, (roll= 8.19 degree, heave = 3.99 m and pitch = 3.50 degrees) were found to be higher to those in the collinear cases. It is worth noting that, in the non-collinear case, the incident wave length effectively increases due to the wave-current interaction, and the length ratio between the FPSO model and wavelength was less than one in the present study leading to the increased wave frequency motions.

Furthermore, the maximum tension in the most critical line (L-1) was found to be 3812.17 kN in the non-collinear case, mainly because of the higher contribution of the coupled surge-sway motion responses while the maximum mean tension was observed in the collinear 'In-line' case (L-1, 2665.07 kN), a clear indication that mooring lines in the non-collinear condition are more sensitive to the dynamic response.

-FPSO model with mooring lines and risers

Table 8 shows the statistical results for the FPSO model complete with mooring lines and risers in the full operational configuration. The non-collinear case also showed slightly higher statistical values for low frequency surge motion (-76.75 m) compared to the results for the collinear 'Between-lines' case (surge = -75.53 m), and a much smaller value (surge = -50.90 m) for the collinear 'In-line' case. The highest motion response in the non-collinear case was mainly attributed to the interaction wave-current load, which increases the mean drift force and slow-drift excitation forces on the FPSO model. For yaw motions, the non-collinear condition tends to induce the highest mean motion (-43.43 degrees) compared with collinear conditions,

as expected. In the case of the wave frequency induced motions of heave, pitch and roll, the non-collinear case also showed the highest values, which can be attributed to the coupled effect from the yaw motions.

The maximum tension in the most loaded mooring line (L-1) was 3598.29 kN, which was observed in the 'In-line' case, whereas the most critical tension in the risers for R1 was 2364.77 kN in the non-collinear case, mainly due to the increase in wave frequency motion.

The influence of the riser system on the maximum motion response and dynamic tension response of the mooring lines for the most critical case (Non-collinear) in Full load condition was tested, and the results are presented in Table 7 and 8. The motion response in surge direction was reduced by 13%, with a standard deviation of 15%. The differences in mean motion response were relatively small when the riser system was considered. The contribution of risers to the maximum response are mainly from the hydrodynamic damping, which decreased the dynamic motion response. The maximum dynamic tension response of the most loaded mooring line (L-1) decreased by 6% and again the difference in mean tension response is neglected when the riser system was considered.

ii. Full load condition vs. Ballast load condition under the non-collinear environment

-FPSO model with mooring lines

The statistical values for the Ballast Load condition of the FPSO model were studied for the non-collinear case only. Table 8 shows that the maximum motion response for the Ballast Load condition in the surge direction (-68.94 m), and the results for the Full load condition (-86.62 m) is found to be considerably larger. The same trend is observed for the mean motion and standard deviation (Figs. 45 to 47). However, the maximum sway motion response (39.57 m) for the Ballast Load condition tends to be marginally larger than that for the Full load condition (34.18 m). This is mainly attributed to the fact that, for the Ballast Load condition, the mean, maximum and minimum values of the yaw response, in terms of absolute values, are higher (41.73, 22.98 and 60.09 degrees, respectively) than those for the Full load condition

(39.30, 20.88 and 54.53 degrees). The relative increases of the yaw motions can be attributed to the larger projected area of the FPSO model exposed to wind for the Ballast Load condition that for the Full load condition, which is due to the differences in the draughts. The higher yaw responses lead to slight increases of the wave frequency motion in roll, heave and pitch for the Ballast Load condition.

The maximum line tension was observed in L-1 (3999.20 kN) for the Ballast Load condition, which is slightly higher than that for Full load condition (3812.17 kN) in the non-collinear environment. This can be attributed to the higher coupled surge and sway motion responses and the differences in the draughts of the FPSO model.

-FPSO model with mooring lines and risers

The maximum motion response for the Ballast Load condition was -63.64 m in the surge, which is smaller than results of -76.75 m for the Full load condition, both in non-collinear environment, as shown in Table 8 and Figs. 45 to 47. In contrast, the maximum motion response in sway (39.61 m) for the Ballast Load condition is similar than that for the Full load condition (39.15 m) in the same non-collinear environment.

For the wave frequency motions, it is noted that the differences in heave, roll and pitch between the Ballast Load condition and Full load condition are small. Furthermore, the maximum critical line tension L-1 (3758.36 kN) for the Ballast Load condition is slightly higher than that for the Full load condition (3585.89 kN), but the maximum tension in the most loaded riser (R-1) (2229.30 kN) for the Ballast Load condition is slightly lower than that for the Full load condition (R-1) (2364.772 kN) in non-collinear environment.

iii. Effects of current and wind

In order to examine the effects of current and wind on the dynamics of the coupled system, comparisons are made for the results obtained under the two collinear 'In-line' cases, i.e., one

582 with irregular waves only and the other with irregular waves, current and wind, (Fig. 48). The
583 statistical values for the surge motions of the FPSO model with mooring lines only were
584 analysed. It was clear that the mean drift motion response increased two-fold for the
585 environment with irregular waves, current and wind compared to that of the system under
586 irregular waves only. Further, the mean drift motion of the FPSO model tends to govern the
587 total motion response when the irregular waves are influenced by wind and current while the
588 dynamic motion (slow drift motion) component is smaller with an average of 18% compared to
589 the FPSO model exposed to irregular waves. This behaviour is mainly due to the collinear
590 wave-current interactions which increase the drift mean forces and the wave-drift damping on
591 the FPSO model (Zhao and Faltinsen, 1989; Faltinsen, 1994; Monroy et al., 2012; Stansberg
592 *et al.*, 2013).

593 On the other hand, the motion response of the FPSO model from current load was slightly
594 higher than the motion response from the wind load, and a small standard deviation was
595 observed for both motions due to the current and wind loads respectively, which confirms that
596 the FPSO system with mooring lines mainly responds to mean motion behaviour. Oscillation
597 loads from the current and wind are insignificant.

598 Fig. 49 shows the comparison of the tension response of the most loaded mooring line (L-
599 1) for both collinear cases with irregular waves only and irregular waves, current and wind.
600 The mean tension response is observed to be 15% higher for the system exposed to irregular
601 waves, current and wind compared to that of the system with irregular waves only. The
602 dynamic tension response of the most loaded mooring line was observed similar in both
603 collinear cases (irregular waves, current and wind, and irregular waves only). It is clear that
604 the dynamics of the system when exposed to a collinear case of irregular waves, current and
605 wind, is dominated by the mean drift motion response of the FPSO model and mean tension
606 response of the mooring lines.

607 The statistical values for the surge motions of the FPSO model with mooring lines only show
608 that, for the non-collinear environment with the irregular waves, current and wind, the mean
609 drift motion response increases by two-fold compared to the system exposed to irregular
610 waves only (Fig. 50). The dynamic motion (slow-drift oscillation) is higher by 27% compared
611 to the system under irregular waves only. The mean tension response of the most loaded
612 mooring line (L-1) for the system exposed to irregular waves, current and wind was observed
613 slightly higher (6%) compared to the system under irregular waves only (Fig. 51). The main
614 difference was observed in the dynamic tension response. The dynamic tension in the most
615 loaded mooring line increases 21% in the system exposed to irregular waves, current and wind
616 than that of the system under irregular waves only. This is a clear indication that wave-current
617 interaction in non-collinear environment has an important effect on both mean drift motion and
618 the slow-drift oscillation of the FPSO model and the dynamic tension of the mooring lines. The
619 reason is that changes in the mean heading of the vessel when comparing collinear and non-
620 collinear conditions influence the mean yaw motion response of the FPSO model. The different
621 yaw motions cause different first-order and second-order motion responses of the FPSO
622 model for the collinear and non-collinear environment condition. Additionally, wave-current
623 interaction changes the fluid flow pattern around of the structure and subsequently impacts on
624 the mean wave loads according to potential theory, and they are connected with the structure's
625 ability to create waves (Faltinsen, 1994).
626
627 **6. Conclusions**
628 Based on the results of the present study, the motion response of the FPSO with mooring
629 and riser system for both the Full load and the Ballast load conditions were observed to be
630 sensitive to the direction of the incident wave. It is confirmed that FPSO system is more critical
631 to the beam and quartering seas. The motion response spectra analysis revealed that risers
632 have a great influence on low-frequency damping, particularly in the surge direction, whereas
633 the damping mainly contributes to roll of the wave frequency motion response. Under the non-
634 collinear environmental condition, the interaction between irregular waves and current

increases the steady wave drift force on the FPSO model compared to the collinear cases. The yaw motion response influences the wave frequency motions (heave, roll, and pitch) of the FPSO under the non-collinear condition. The impact of the FPSO loading condition on the wave frequency motions is found to be insignificant. The highest tension response in the mooring lines is observed in the Ballast load condition for the non-collinear case due to a higher coupled surge and sway motion response and less draught on the FPSO. The tensions in the risers is slightly higher in the non-collinear environment for the Full load condition and the wave frequency motions are sensitive to risers. The changes in the mean heading of the vessel when comparing collinear and non-collinear conditions influence the mean yaw motion response of the FPSO model. The different mean yaw motions cause different first-order and second-order motion responses of the FPSO model for the collinear and non-collinear environment condition.

Interaction between waves, current and wind in collinear environment increases the mean drift motion response and reduces the slow-drift oscillation response of the FPSO model due to the increase of the drift damping compared to irregular waves only. However, interaction of waves, current and wind in non-collinear environment is more complex which tends to increase the mean drift motion, the drift damping and the slow-drift oscillation response of the FPSO model compared to the system exposed to irregular waves only. Based on the present experiment results confirms that the non-collinear environmental conditions are important in the analysis and design of the hydrodynamic performance of the FPSO with mooring and riser systems.

Acknowledgments

The authors would like to thank the CONACYT-SENER-MEXICO, Pemex Exploration and Production PEMEX, Newcastle University and Shanghai Jiao Tong University for their support. The authors would like to acknowledge the support by British Council (China) under “Sino-UK Higher Education Research Partnership” scheme.

References

1. API-RP-2SK, 2005. Recommended practice for design and analysis of stationkeeping systems for floating structures: exploration and production department. API recommended practice 2SK (RP 2SK), 3rd edition, American Petroleum Institute, Washinton, DC.
2. Arun Kr. DEV, Viscous effects in drift forces on semi-submersibles. Delft University, The Netherlands, 1996.
3. Baar, J.J.M., Heyl, C.N. and Rodenbusch, G., 2000. Extreme response of turret moored tankers. 32nd Annual Offshore Technology Conference, Paper OTC-12147-MS, Houston, Texas, Vol. 2, pp. 749-759.
4. Baarholm, R., Fylling, I., Stansberg, C.T. and Oritsland, O., 2006. Model testing of ultra-deepwater floater systems: Truncation and software verification methodology. Proceedings of 25th International Conference on Offshore Mechanics and Arctic Engineering, Paper OMAE2006-92492, Hamburg, Germany, Vol 1, pp. 527-537.
5. BMT, 2000. Review of model testing requirements for FPSO's. BMT Fluid Mechanics Ltd. Offshore Technology Report 2000/123, Teddington, United Kingdom.
6. Chakrabarti, S.K., 1994. Offshore structure modeling. Advanced Series on Ocean Engineering, Volume 9, pp. 445-451.
7. Chakrabarti, S., 1998. Physical model testing of floating offshore structures. Proceedings of MTS Dynamic Positioning Conference, Houston, USA, pp. 1-33.
8. Chakrabarti, S.K., 2005. Technical editor. Handbook of Offshore Engineering, Elsevier Publications, Oxford, UK.
9. Faltinsen, O., 1994. Wave and current induced motions of floading production systems. Elsevier, Applied Ocean Research, 15, pp. 351-370.
10. Faltinsen, O.M., 1990. Wave loads on offshore structures. Annual Review of Fluid Mechanics, 22, pp. 35-56.

689 11. Fylling, I.J., Stansberg, C. T., 2005. Model testing of deepwater floating production
690 systems: Strategy for truncation of moorings and risers. Proceedings of 17th DOT
691 Conference, Vitoria, Brazil, pp. 1-4.
692 12. Irani, M.B., Johnson R. P. and Ward E. G., 2001. FPSO responses to wind, wave and
693 current loading. Proceedings of 20th International Conference on Offshore Mechanics
694 and Arctic Engineering, Paper OMAE2001/OFT-1023, Rio de Janeiro, Brazil, Vol.1 pp.
695 57-66.
696 13. ITTC, 2008. Recommended procedures and guidelines, testing and extrapolation
697 methods, loads and responses. Truncation of test models and integration with numerical
698 simulations ITTC-07-3.5. Ocean Engineering Committee of 25th ITTC, Fukuoka, Japan.
699 14. Luo, Y., Baudic, S., Poranski, P., Wichers, J., Stansberg, C.T. and Ormberg, H., 2004.
700 Deepstar study on predicting FPSO responses—model tests vs numerical analysis.
701 Offshore Technology Conference, paper OTC-16585, Houston Texas.
702 15. Monroy, C., Giorgiutti, Y. and Chen, X.-B., 2012. First and second order wave-current
703 interactions for floating bodies. Proceedings of 31st International Conference on Ocean,
704 Offshore and Arctic Engineering, OMAE2012-83409, Rio de Janeiro Brazil, Vol. 1,
705 pp.373-382.
706 16. Moxnes, S. Larsen, K., 1998. Ultra small scale model testing of a FPSO ship.
707 Proceedings of the 17th International Offshore Mechanics and Arctic Engineering,
708 OMAE98-0381, Lisbon, Portugal.
709 17. Qualisys, 2010. Contactless optical tracking motion system Qualisys, Gothenburg,
710 Sweden.
711 18. Stansberg, C.T., Hoff, J.R., Hermundstad, E.M. and Baarholm, R., 2013. Wave drift
712 forces and responses in current. Proceedings of 32nd International Conference on
713 Ocean, Offshore and Arctic Engineering, OMAE2013-11407, Nantes, France, Vol. 1, pp.
714 V001T01A071.

19. Stansberg, C.T., Karlsen, S.I., Ward, E.G., Wichers, J.E.W. and Irani, M.B., 2004. Model testing for ultradeep waters. Offshore Technology Conference, paper OTC-16587, Houston Texas.

20. Stansberg, C.T., Øritsland, O. and Kleiven, G., 2000. VERIDEEP: Reliable methods for laboratory verification of mooring and stationkeeping in deep water. Offshore Technology Conference, paper OTC-12087, Houston Texas.

21. Stansberg, C.T., Ormberg, H. and Oritsland, O., 2002. Challenges in deep water experiments: Hybrid approach. Journal of Offshore Mechanics and Arctic Engineering, 124(2), pp. 90-96.

22. Su, Y., Yang, J., Xiao, L. and Chen, G., 2009. Experimental and numerical study on large truncation of deepwater mooring line. Proceedings 28th International Conference on Ocean, Offshore and Arctic Engineering, OMAE2009-79218, Honolulu, Hawaii, USA, pp. 201-212.

23. Tahar, A., Kim, M. H., 2003. Hull/mooring/riser coupled dynamic analysis and sensitivity study of a tanker-based FPSO. Applied Ocean Research, 25(6), pp. 367-382.

24. Waals, O., Van D., Radboud R.T, 2004. Truncation methods for deep water mooring systems for a catenary moored FPSO and a semi taut moored semisubmersible, DOT2004, paper 24-1, New Orleans, USA.

25. SESAM, 2014. Frequency domain hydrodynamic analysis of stationary vessels, Wadam-Hydro-D. Wadam User Manual, DnV software.

26. Ward, E.G., Irani, M.B. and Johnson, R.P., 2001. Responses of a tanker-based FPSO to hurricanes. Offshore Technology Conference, paper OTC-3214-MS, Houston, Texas.

27. Zhao, R. and Faltinsen, O.M., 1989. Interaction between current, waves and marine structures. 5th International Conference on Ship Hydrodynamics Hiroshima, pp. 513-27.

List of Tables

List of Figures

787

788 **Fig. 31.** Surge motion response spectra, non-collinear Case for the Full load condition

789 **Fig. 32**. Roll motion spectra, Non-collinear case for the Full load condition

790 **Fig. 33**. Line tension response spectra for the Full load condition

791 **Fig. 34**. Riser tension response spectra for the Full load condition

792 **Fig. 35**. Surge motion response spectra for Full and Ballast load condition

793 **Fig. 36**. Line tension response spectra for the Full and Ballast load condition

794 **Fig. 37.** Offsets trajectories of the FPSO with mooring lines and risers, non-collinear case Full Load condition

795 **Fig. 38.** Yaw motion response of the FPSO with mooring lines and risers, non-collinear case Full Load condition

796 **Fig. 39.** Offsets trajectories of the FPSO with mooring lines, non-collinear case Full Load condition

797 **Fig. 40.** Yaw motion response of the FPSO with mooring lines, non-collinear case Full Load condition

798 **Fig. 41.** Offsets trajectories of the FPSO with mooring lines, non-collinear case Ballast Load condition

799 **Fig. 42.** Yaw motion response of the FPSO with mooring lines, non-collinear case Ballast Load condition

800 **Fig. 43.** Offsets trajectories of the FPSO with mooring lines and risers, non-collinear case Ballast Load condition

801 **Fig. 44.** Yaw motion response of the FPSO with mooring lines and risers, non-collinear case Ballast Load condition

802 **Fig. 45**. Comparison of the extreme surge motion FPSO mooring lines (Case B) vs. FPSO mooring lines and riser
803 (Case C) for the Full load and Ballast load conditions (in terms of absolute values)

804 **Fig. 46**. Comparison of the mean surge motion FPSO mooring lines (Case B) vs. FPSO mooring lines and riser
805 (Case C) for the Full load and Ballast load conditions (in terms of absolute values)

806 **Fig. 47**. Comparison of the standard deviation of surge motion FPSO mooring lines (Case B) vs. FPSO mooring
807 lines and riser (Case C) for the Full load and Ballast load

808 **Fig. 48**. Statistical values of surge motion responses for the Collinear 'In-line' cases for the FPSO with mooring
809 lines exposed to irregular waves only and irregular waves, current and wind.

810 **Fig. 49**. Statistical values of tension response of the loaded line (L-1) for the Collinear 'In-line' cases for the FPSO
811 with mooring lines exposed to irregular waves only and irregular waves, current and wind.

812 **Fig. 50**. Statistical values of surge motion responses for the Collinear 'In-line' case exposed to irregular waves only
813 and Non-Collinear cases exposed to irregular waves, current and wind, FPSO model with mooring lines

814 **Fig. 51**. Statistical values of tension response of the loaded line (L-1) for the Collinear 'In-line' and Non-collinear
815 cases for the FPSO with mooring lines exposed to irregular waves only and irregular waves, current and wind.

816

817

818 **Table 1**

819 Prototype and model scale dimensions and characteristics of the FPSO

Full load Condition			Ballast load Condition	
Description	Prototype	Model Scale	Prototype	Model Scale
Length LPP (m)	300	4.69	300	4.69
Breadth, B (m)	46.20	0.72	46.20	0.72
Depth, H (m)	26.20	0.41	26.20	0.41
Draught, T (m)	16.50	0.26	9.00	0.14
Ta (m)	16.50	0.26	9.50	0.15
Tf (m)	16.50	0.26	8.50	0.13
Length/Beam ratio (L/B)	6.49	0.10	6.49	0.10
Beam/Draught ratio (B/T)	2.80	0.04	5.13	0.08
Displacement (tonnes)	218876	0.82	122530	0.46
XB, XG (m)	2.43	0.04	3.08	0.05
ZG (m)	11.43	0.18	7.87	0.12`
Kxx (m)	16.17	0.25	20.79	0.33
Kyy (m)	86.72	1.36	86.72	1.36

820

821

822

823 **Table 2**

824 Mooring line characteristics

Description	Prototype	Truncate Specification
Number of mooring lines	9	9
Pretension (kN)	2025	2025
Total Length of mooring line (m)	2185	1160
Segment 1: Fairlead chain	R4S Studless	
Length (m)	50	50
Diameter (mm)	90	90
Mass in water (tonnes/m)	0.146	0.146
EA (kN)	691740	691740
Breaking strength (kN)	8167	-
Segment 2: Mid-section	Spiral Strand	
Length (m)	1200	580
Diameter (mm)	90	90
Mass in water (tonnes/m)	0.0336	0.116
EA (kN)	766000	68000
Breaking strength (kN)	7938	-
Segment 3: Chain ground section	R4S Studless	
Length (m)	935	530
Diameter (mm)	90	90
Mass in water (tonnes/m)	0.146	0.133
EA (kN)	691740	60000
Breaking strength (kN)	8167	-

825

826

827 **Table 3**

828 Riser characteristics

829

Description	Prototype	Truncate Specification
Number of risers	6 symmetric	6 symmetric
Pretension (kN)	1500	1500
Total length of riser (m)	2650	1400
Outside diameter (mm)	273	273
Inside diameter (mm)	235	235
Mass in water (tonnes/m)	0.096	0.234
EA (kN)	3039364	85000
Specification	API-5L-X-65	

835

836

837 **Table 4**

838 Storm environmental conditions

Description	Unit	Storm environment condition
Waves		
Hs	m	9.67
Tp	s	13.28
Wave spectrum	Jonswap (γ=2.3)	
Wave direction	deg	180^0
Wind speed (1-hr)	m/s	21.95
Wind spectrum	API RP 2A-WSD	
Wind direction	deg	0^0 and 60^0 of the wave
Surface current	m/s	1.44
Current direction	deg	0^0 and 90^0 of wave

839

840

841

842 **Table 5**

843 Natural periods and damping ratio of six DOF for Full load and Ballast load conditions

DOF	Full load			Ballast load		
	T_n (s)	Damping ratio	Added mass coeff.	T_n (s)	Damping ratio	Added mass coeff.
Surge	223.58	0.015	-	168.56	0.013	-
Sway	277.39	0.030	-	184.21	0.040	-
Heave	11.55	0.130	1.06	11.15	0.120	2.11
Roll	13.21	0.020	0.17	11.23	0.030	0.14
Pitch	11.60	0.100	0.95	10.38	0.210	1.53
Yaw	166.90	0.030	-	119.66	0.013	-

844

845

846

847 **Table 6**

848 Natural periods and total damping ratio of the free decay tests of the FPSO model, mooring lines and risers for

849 the 'In-line' and 'Between-lines' cases in the surge direction, in the Full load condition.

Parameters	Only FPSO	FPSO+Mooring lines 'In-line' Case	FPSO+Mooring lines 'Between-Lines' Case	FPSO+Mooring lines+Risers 'In-line' Case	FPSO+Mooring lines+Risers 'Between-Lines' Case
Periods (s)	223.81 s	353.57 s	362.05 s	339.35 s	344.18 s
Damping ratio	0.015	0.030	0.028	0.043	0.034

850

851

852

853 **Table 7**

854 Statistical values of the motions in the Full load and Ballast load conditions for the Collinear and the Non-Collinear

855 cases for the FPSO model with mooring lines

856

FPSO vessel and Mooring lines "CASE B" Environment condition: Irregular Wave-Current-Wind					
Description	FPSO Full load Condition				FPSO Ballast load Condition
	Statistical	Collinear 'In-line' Case	Collinear 'Between-lines' Case	Non-Collinear Case	Non-Collinear Case
Surge (m)	Max	-3.92	-3.02	-3.38	-10.83
	Min	-56.93	-84.46	-86.62	-68.94
	Mean	-28.86	-35.67	-43.24	-37.09
	Stdv	9.16	12.31	12.64	9.05
Sway (m)	Max	14.88	15.83	34.18	39.57
	Min	-14.48	-18.11	-16.85	-28.92
	Mean	0.33	-1.53	5.66	1.06
	Stdv	6.14	6.49	10.15	10.84
Heave (m)	Max	2.07	2.24	2.50	3.47
	Min	-2.37	-2.60	-3.99	-4.01
	Mean	-0.11	-0.102	-0.44	-0.29
	Stdv	0.60	0.60	1.00	1.06
Roll (deg)	Max	2.90	2.66	6.49	7.56
	Min	-2.83	-2.83	-8.19	-8.20
	Mean	0.09	0.02	-0.34	-0.21
	Stdv	0.70	0.65	2.01	2.06
Pitch (deg)	Max	3.09	2.87	3.50	4.12
	Min	-2.90	-2.71	-3.18	-3.73
	Mean	0.02	0.02	0.05	0.05
	Stdv	0.804	0.78	1.14	1.23
Yaw (deg)	Max	6.10	5.97	20.88	22.98
	Min	-17.58	-15.03	54.53	60.09
	Mean	-5.14	-3.47	39.30	41.73
	Stdv	4.94	3.89	5.52	5.91
Critical tension line (kN)		L-1	L-7	L-1	L-1
	Max	3729.23	3612.74	3812.17	3999.20
	Min	1915.24	1873.03	1619.00	1766.53
	Mean	2665.07	2451.97	2446.61	2467.93
	Stdv	276.84	220.48	311.49	282.00

857

858

859

860 **Table 8**

861 Statistical values of the motions in the Full load and Ballast load conditions for the Collinear and the Non-Collinear
862 cases for the FPSO model complete with mooring lines and risers

863

FPSO, Mooring lines and Risers "CASE C" Environment condition: Irregular Wave-Current-Wind					
Description	FPSO Full load Condition				FPSO Ballast load Condition
	Statistical	Collinear 'In-line' Case	Collinear 'Between-lines' Case	Non-Collinear Case	Non-Collinear Case
Surge (m)	Max	1.02	-5.76	-10.43	-14.20
	Min	-50.90	-75.53	-76.75	-63.64
	Mean	-22.56	-33.28	-42.09	-33.32
	Stdv	8.49	11.40	10.97	8.12
Sway (m)	Max	25.03	5.25	22.07	39.61
	Min	-14.64	-29.10	-39.15	-19.90
	Mean	0.68	-12.29	-11.89	9.51
	Stdv	7.32	7.98	10.13	10.32
Heave (m)	Max	2.19	2.64	3.65	3.04
	Min	-2.53	-2.50	-4.27	-4.07
	Mean	-0.15	-0.10	-0.31	-0.51
	Stdv	0.59	0.60	1.09	0.84
Roll (deg)	Max	4.48	2.94	6.01	6.04
	Min	-3.93	-2.77	-7.20	-6.80
	Mean	0.06	0.03	-0.32	-0.29
	Stdv	0.71	0.70	1.95	1.66
Pitch (deg)	Max	3.11	3.13	4.11	4.17
	Min	-3.04	-2.90	-4.22	-3.84
	Mean	0.02	0.03	0.03	0.14
	Stdv	0.79	0.80	1.20	1.15
Yaw (deg)	Max	5.72	8.38	29.40	7.29
	Min	-26.45	-11.83	59.67	69.07
	Mean	-6.37	-0.748	43.43	49.68
	Stdv	4.40	4.11	5.36	5.55
Critical tension line (kN)		L-1	L-7	L-1	L-1
	Max	3598.29	3313.35	3585.89	3758.36
	Min	1802.29	1846.79	1692.26	1677.92
	Mean	2508.06	2413.59	2431.79	2485.05
	Stdv	253.64	194.85	281.88	278.24
Riser tension (kN)		R-1	R-4	R-1	R-1
	Max	2127.60	2147.79	2364.77	2229.30
	Min	943.00	978.26	806.74	905.77
	Mean	1499.15	1544.38	1542.06	1547.68
	Stdv	161.81	152.77	226.61	203.59

864

865
866

867

Fig. 1a. FPSO model at scale 1/64th

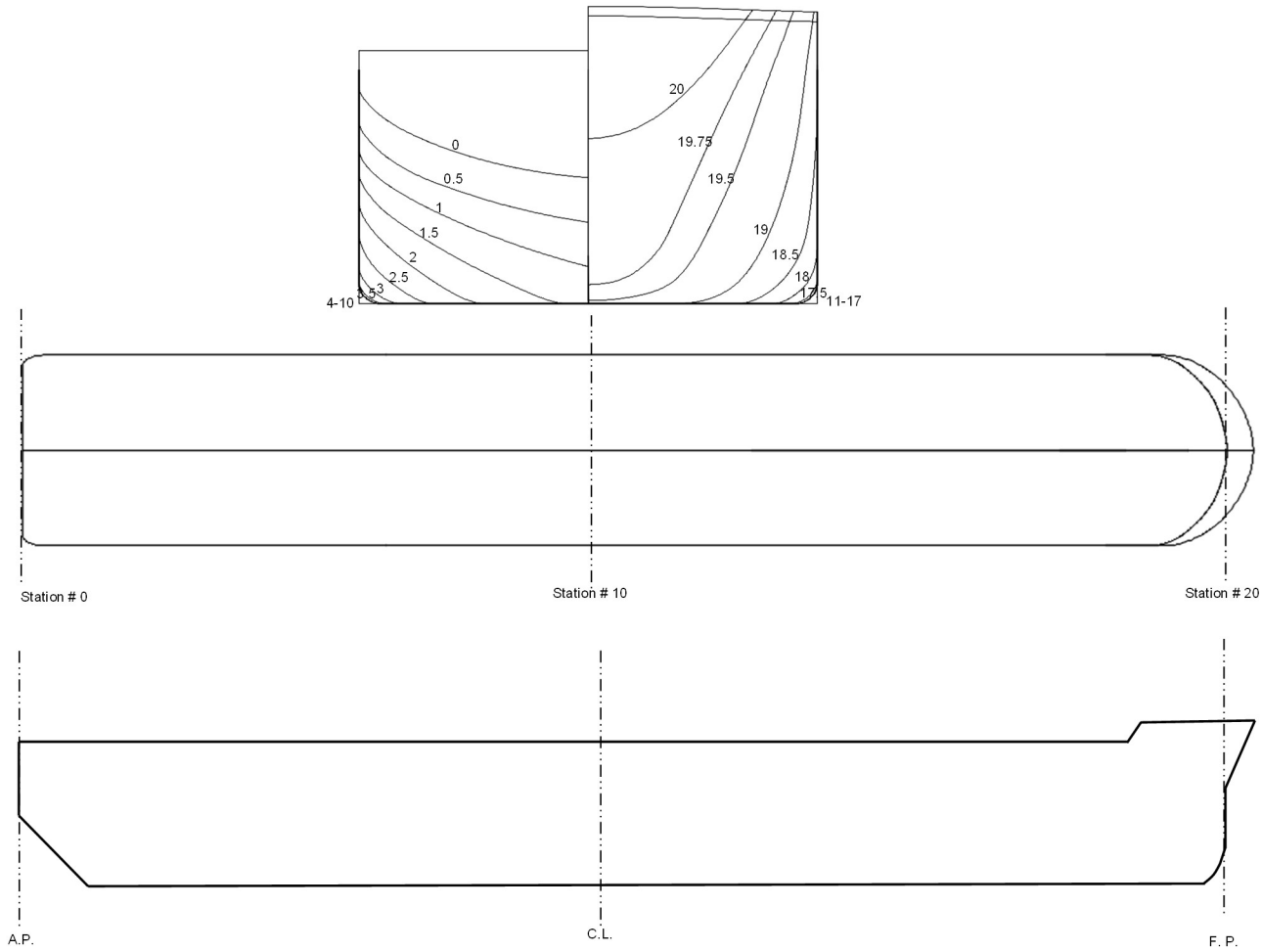

871

872 **Fig. 1b.** Body plan and outline form of the FPSO model

873

874

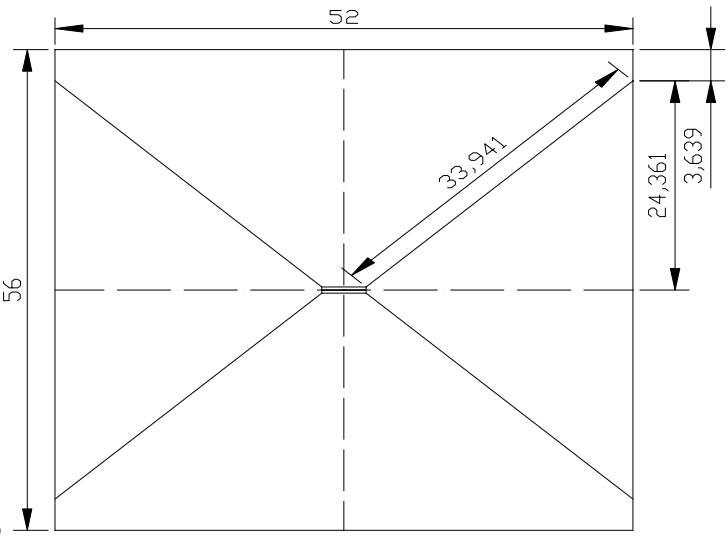

“Case A”

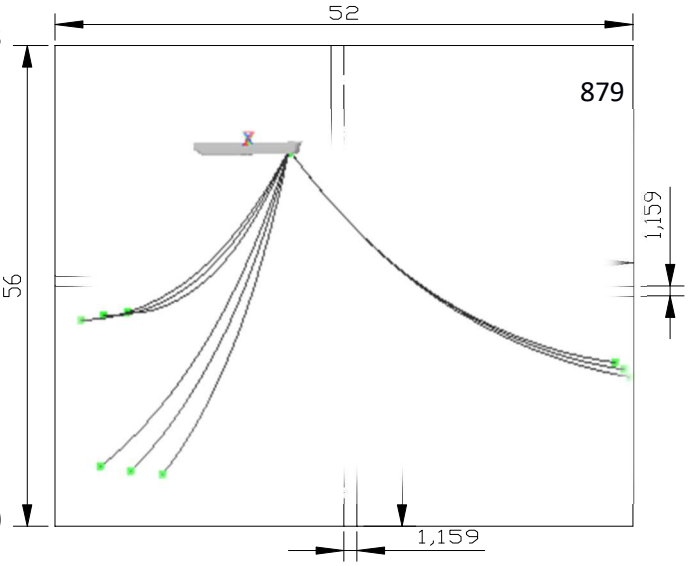

“Case B”

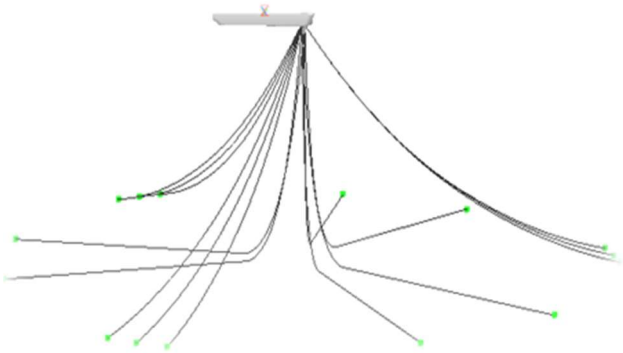

“ “Case C”

Fig. 2. Experimental test configurations, “Case A”, “Case B” and “Case C”

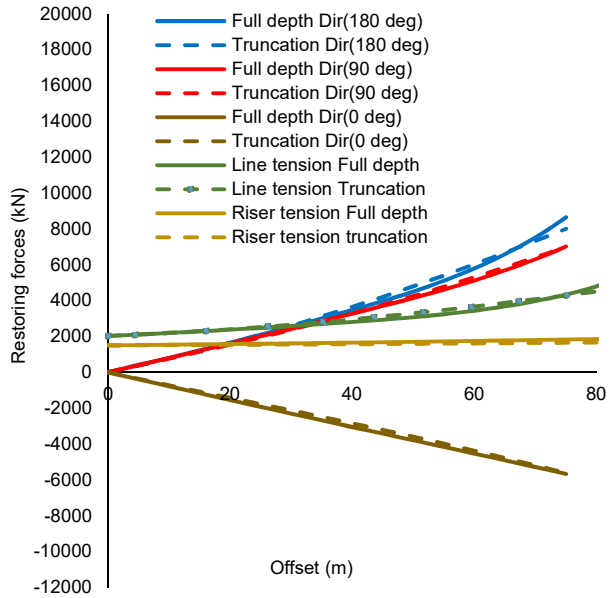

888
889 (a) Restoring forces vs offset

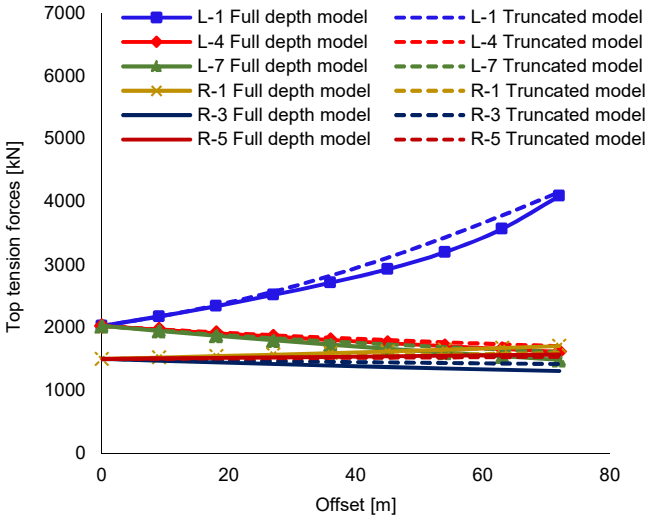

890
891 (b) Top tension forces vs offset

892
893 **Fig. 3.** Mooring line and riser restoring forces and top tension forces of the truncated model and the full depth
894 prototype model

895

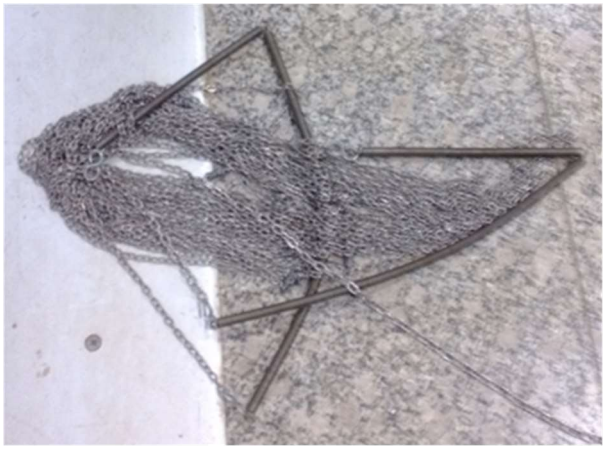

Fig. 4. Mooring lines model at scale 1:64

Fig. 5. Riser model at scale 1:64

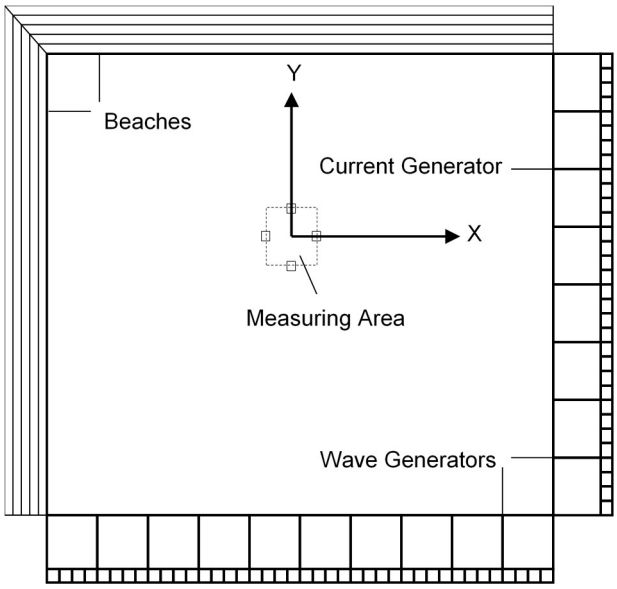

906

907 **Fig. 6.** Plan view of the deepwater offshore basin at SJTU

908

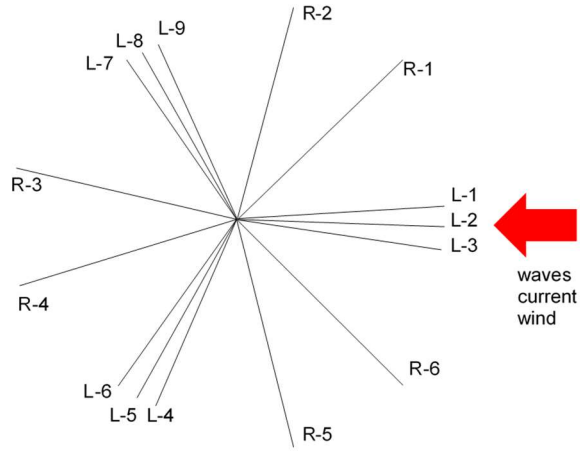

(a) Collinear ‘In-line’

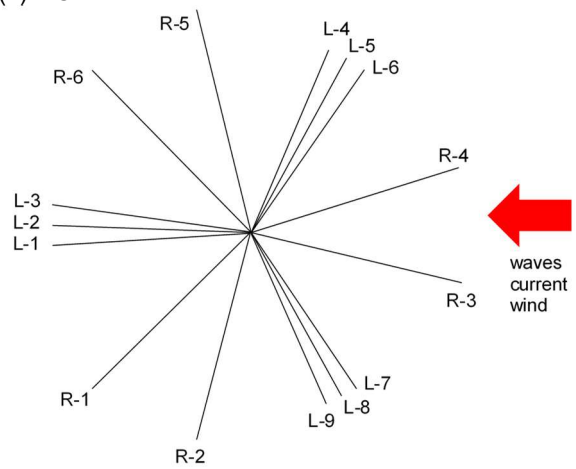

(b) Collinear ‘Between-lines’

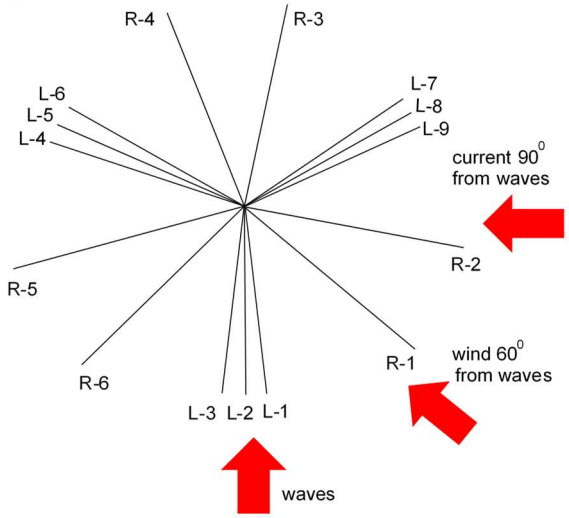

(c) Non-collinear

Fig. 7. (a) Collinear ‘In-line’ and (b) ‘Between-lines’ and (c) Non-collinear (relative to the mooring lines) environmental loading condition. Note: L- Mooring lines R-Risers

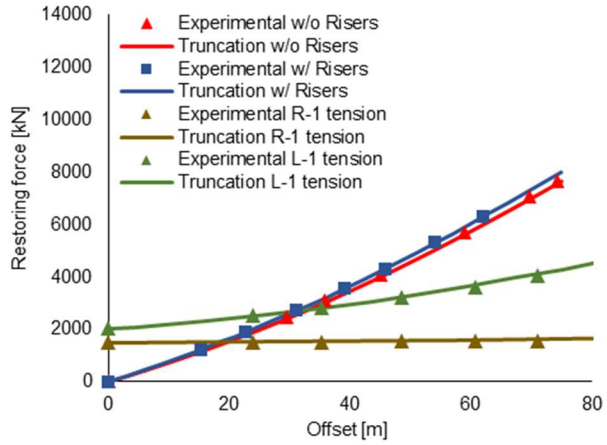

920

921 **Fig. 8.** Restoring forces and offset characteristics in the direction (180^0) (forward direction)

922

923

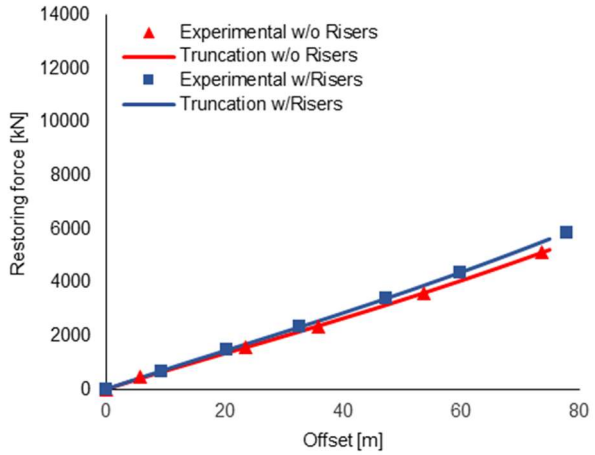

924

925 **Fig. 9.** Restoring forces and offset characteristics in the direction (0^0) (aftward direction)

926

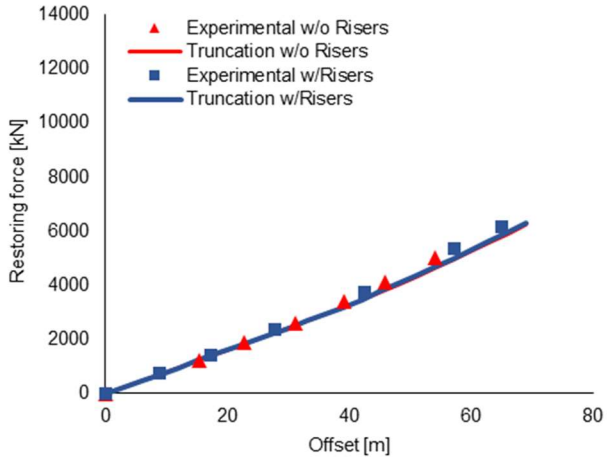

927

928 **Fig. 10.** Restoring forces and offset characteristics in the transverse direction (90^0)

929

930

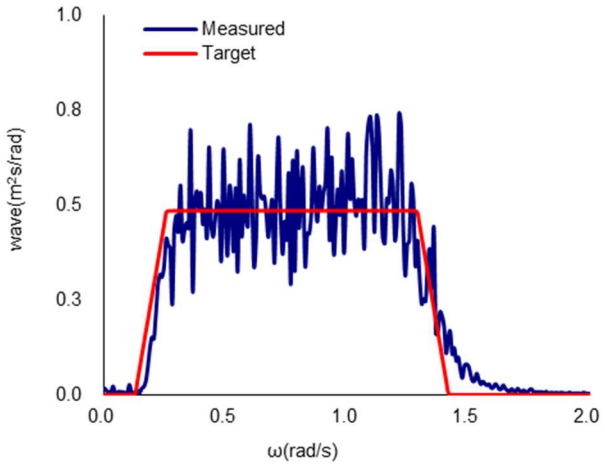

931

932 **Fig. 11.** White noise wave calibration

933

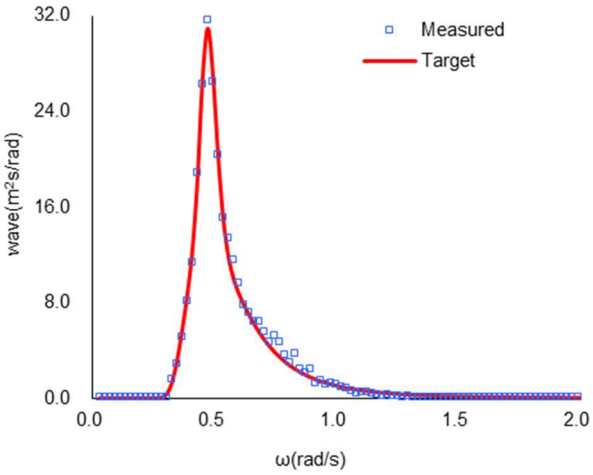

Fig. 12. Irregular wave calibration, direction 180 degrees

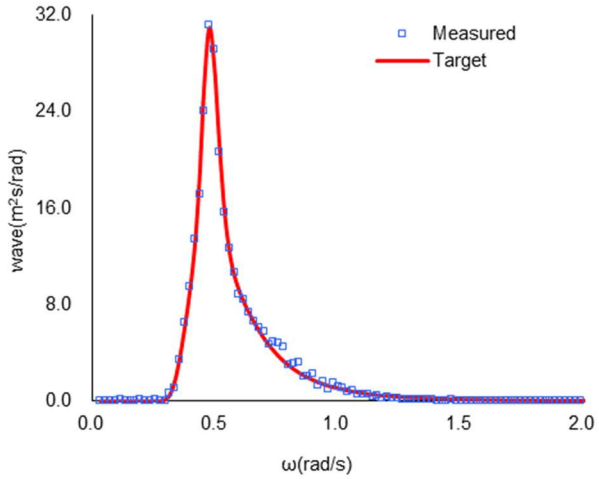

Fig. 13. Irregular waves calibration, direction 90 degrees

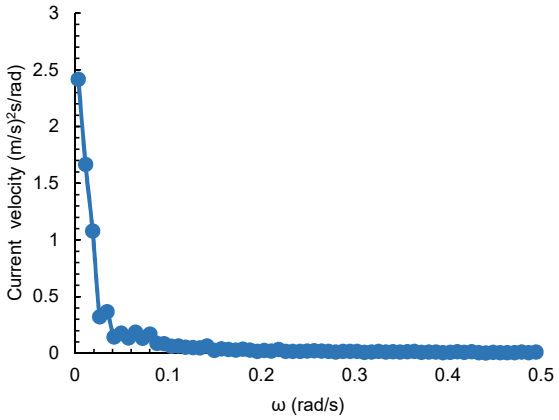

Fig. 14. Spectrum of the calibrated current velocity

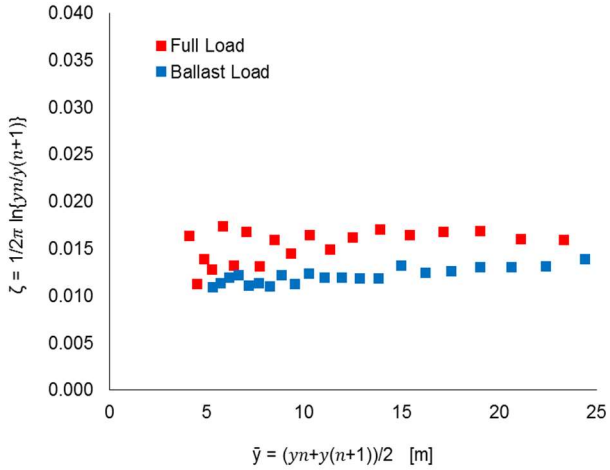

952
953 **Fig. 15.** Surge damping ratios of the horizontal plane motions of the FPSO model

954

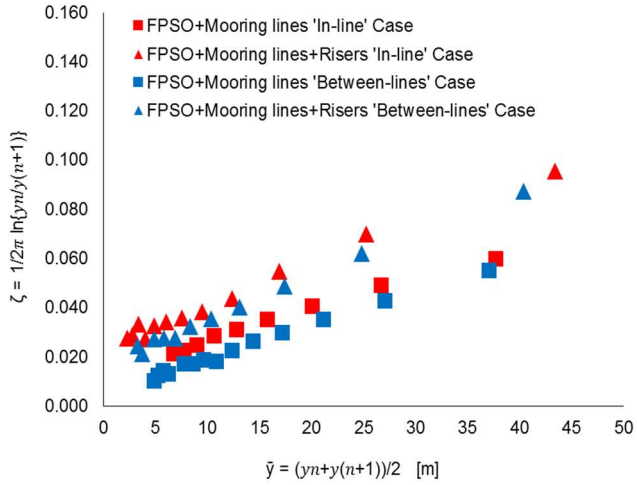

955

956 **Fig. 16.** Damping ratios for surge decay test of the FPSO model, truncated mooring lines and risers for the 'In-line'
957 and 'Between-lines' cases for the Full load condition

958

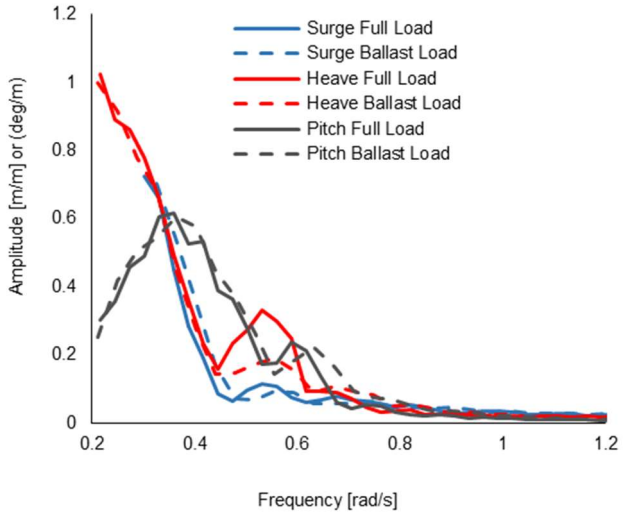

959

960 **Fig. 17.** Surge, Heave and Pitch RAOs of the FPSO model for head seas condition

961

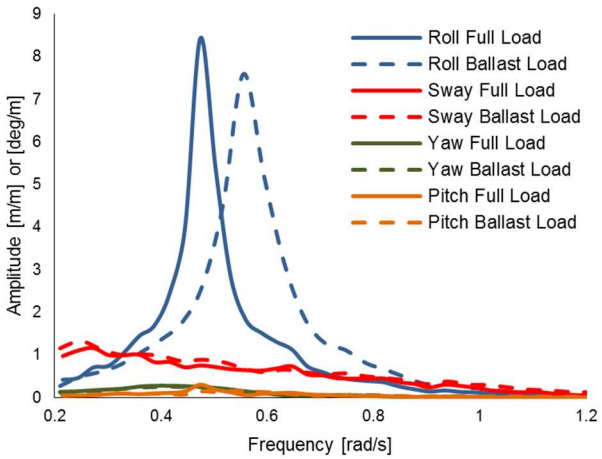

962

963 **Fig. 18.** Roll, Sway, Pitch and Yaw RAOs of the FPSO model for beam seas condition

964

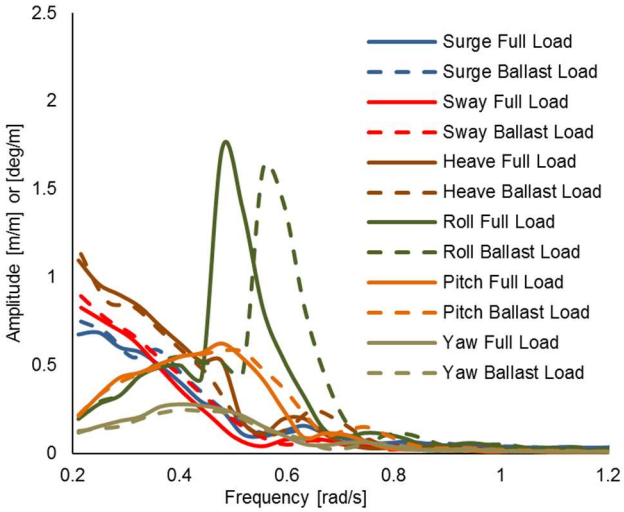

965

966 **Fig. 19.** Surge, Sway, Heave, Roll, Pitch and Yaw RAOs of the FPSO model for quartering seas condition

967

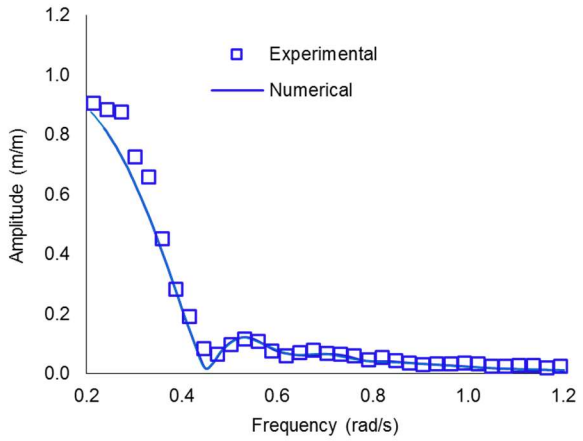

968

969 **Fig. 20**. Surge RAOs for Full Load condition (Head condition)

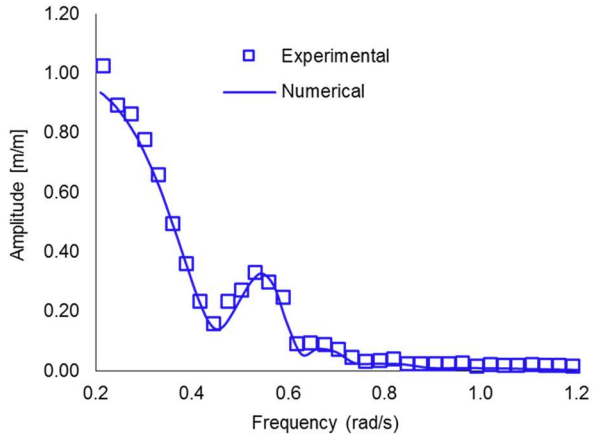

970

971 **Fig. 21**. Heave RAOs for Full Load condition (Head condition)

972

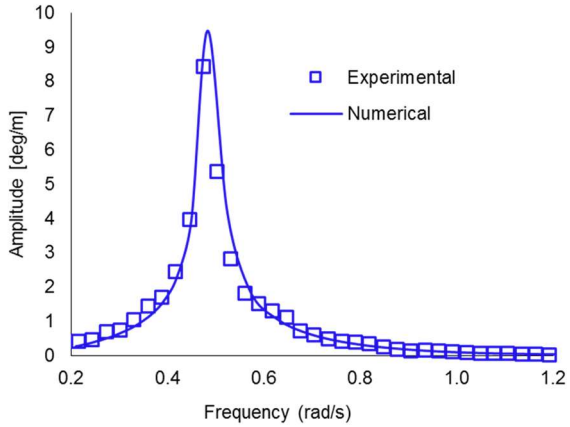

973

974 **Fig. 22**. Roll RAOs for Full Load condition (Beam condition)

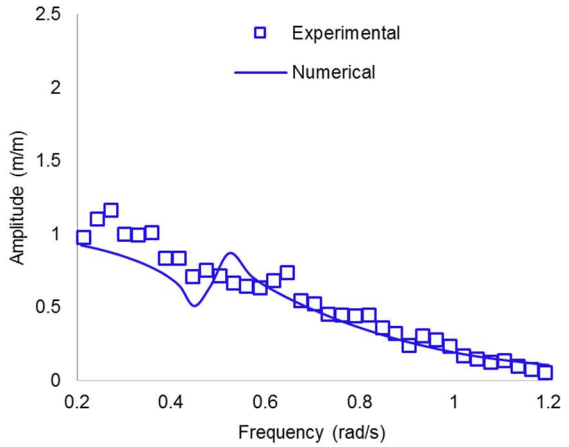

975

976 **Fig. 23**. Sway RAOs for Full Load condition (Beam condition)

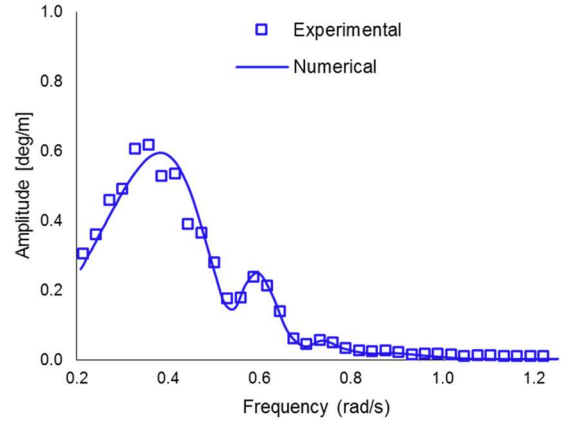

977

978 **Fig. 24**. Pitch RAOs for Full Load condition (Head condition)

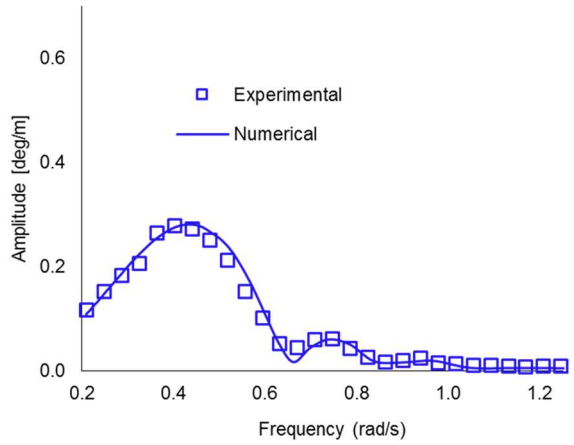

979

980 **Fig. 25**. Yaw RAOs for Full Load condition (Quartering condition)

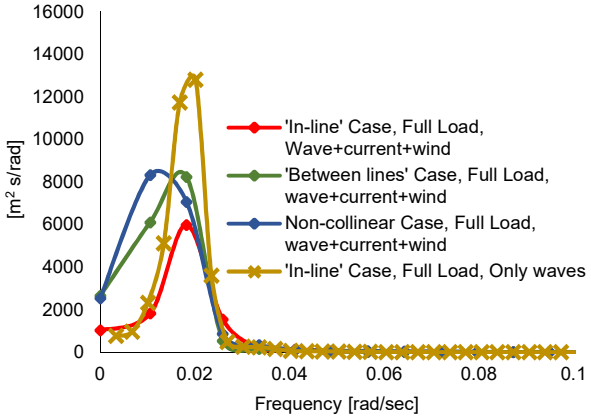

Fig. 26. Surge motion response spectra for the Full load condition

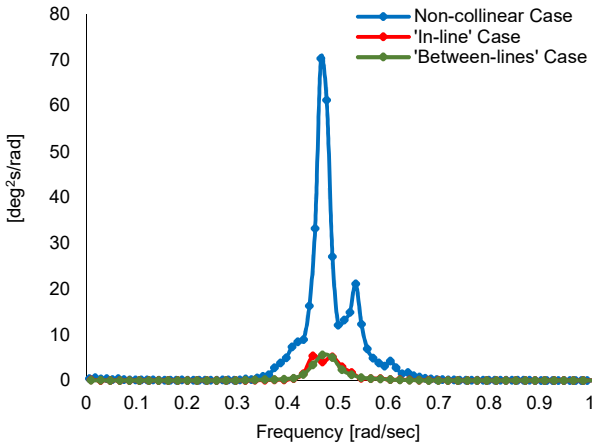

986

987 **Fig. 27.** Roll motion response spectra for the Full load condition

988

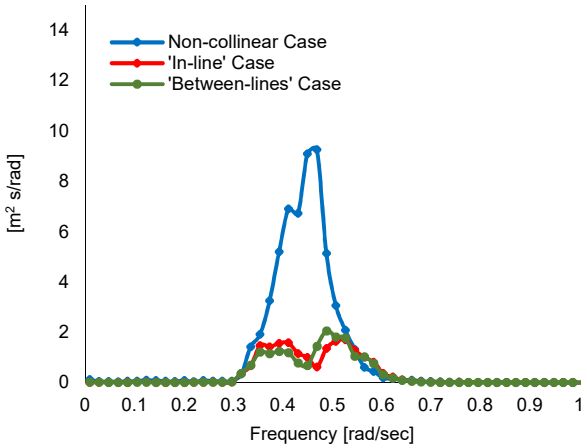

989

990

991 **Fig. 28.** Heave motion response spectra for the Full load condition

992

993

994

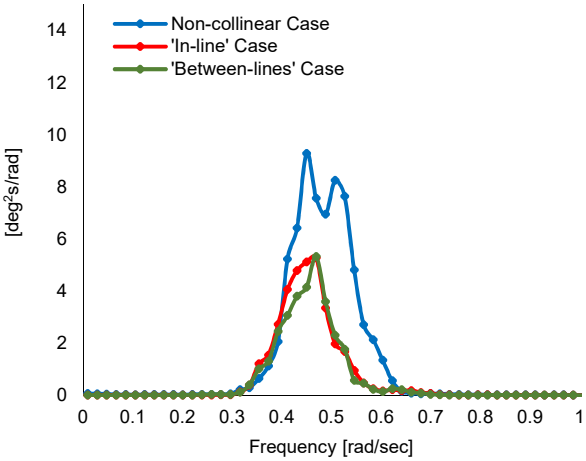

995

996 **Fig. 29.** Pitch motion response spectra for the Full load condition

997

998

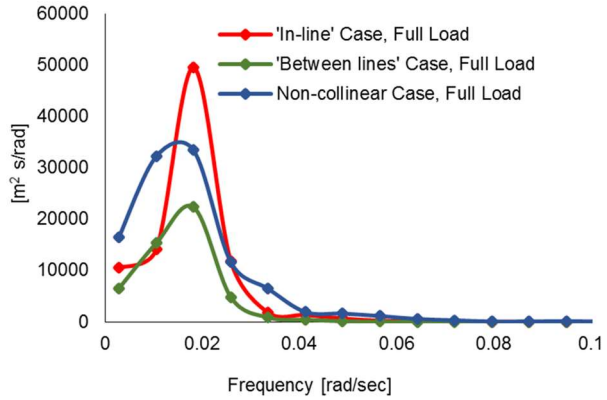

999

1000 **Fig. 30.** Line tension response spectra for the Full load condition

1001

1002

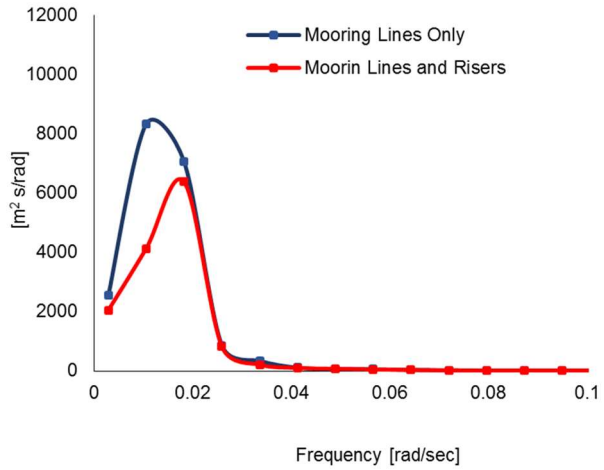

1003

1004 **Fig. 31.** Surge motion response spectra, non-collinear Case for the Full load condition

1005

1006

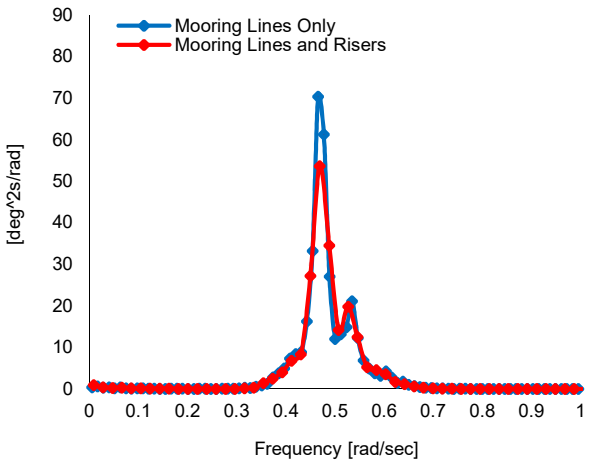

1007

1008 **Fig. 32.** Roll motion spectra, Non-collinear case for the Full load condition

1009

1010

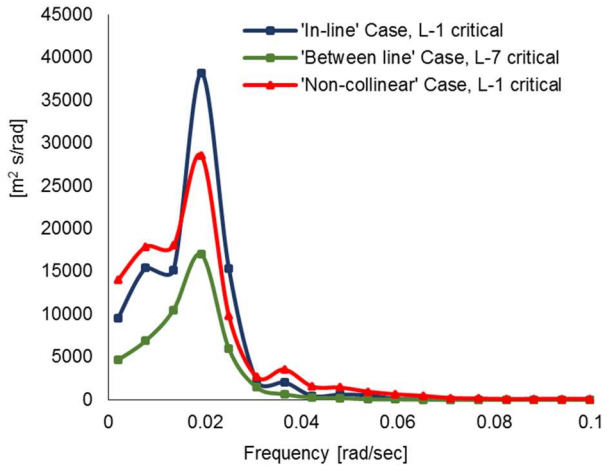

1011

1012 **Fig. 33.** Line tension response spectra for the Full load condition

1013

1014

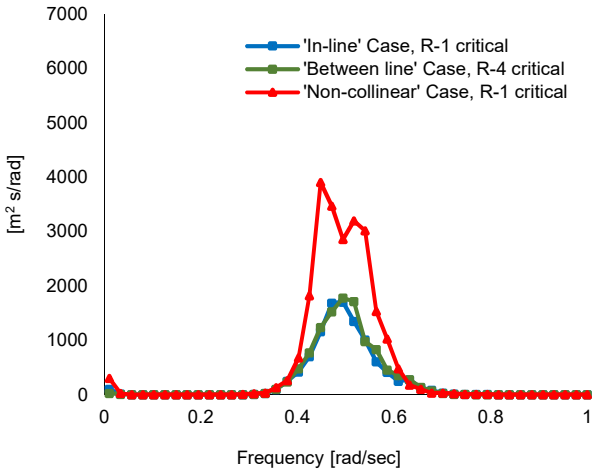

1015

1016 **Fig. 34.** Riser tension response spectra for the Full load condition

1017

1018

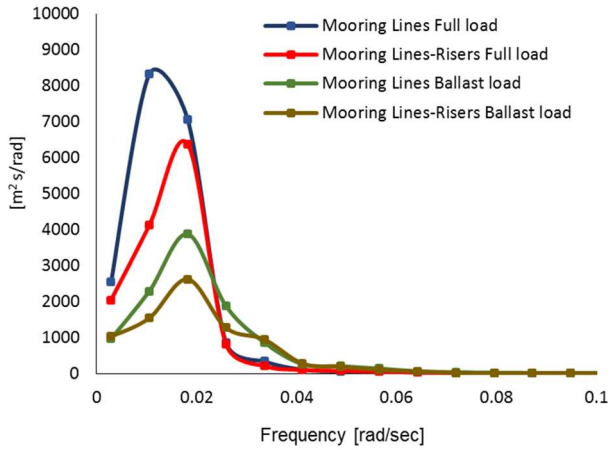

1019

1020 **Fig. 35.** Surge motion response spectra for Full and Ballast load condition

1021

1022

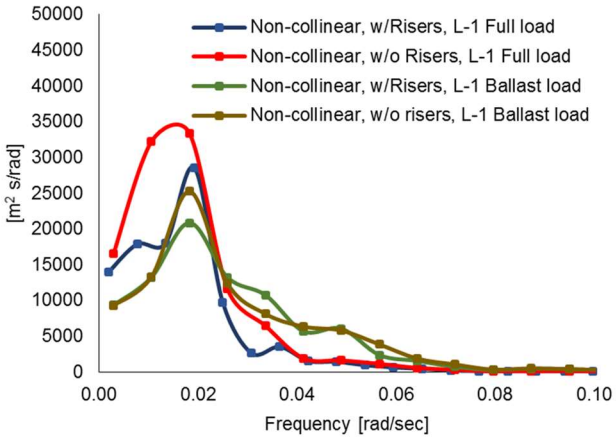

1023

1024 **Fig. 36.** Line tension response spectra for the Full and Ballast load condition

1025

1026

1027

1028

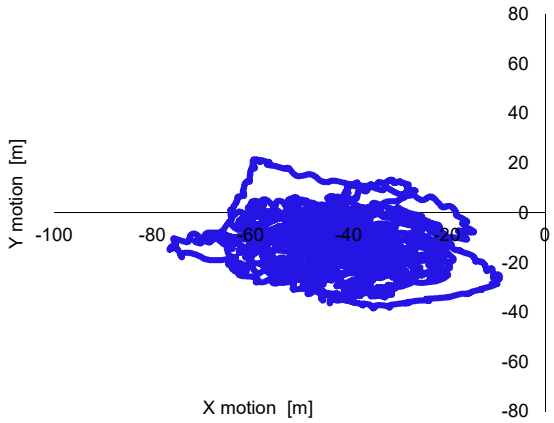

1029

1030

1031 **Fig. 37.** Offsets trajectories of the FPSO with mooring lines

1032 and risers, non-collinear case Full Load condition

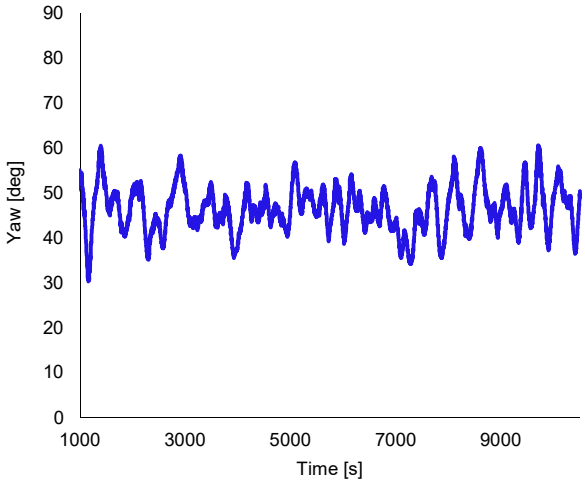

1033

1034 **Fig. 38.** Yaw motion response of the FPSO with mooring lines

1035 and risers, non-collinear case Full Load condition

1036

1037

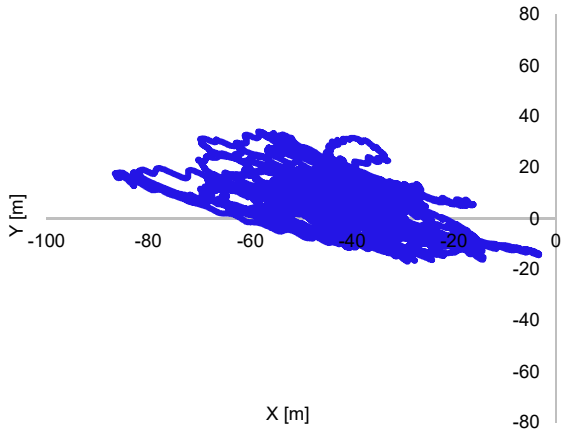

1038

1039 **Fig. 39.** Offsets trajectories of the FPSO with mooring

1040 lines, non-collinear case Full Load condition

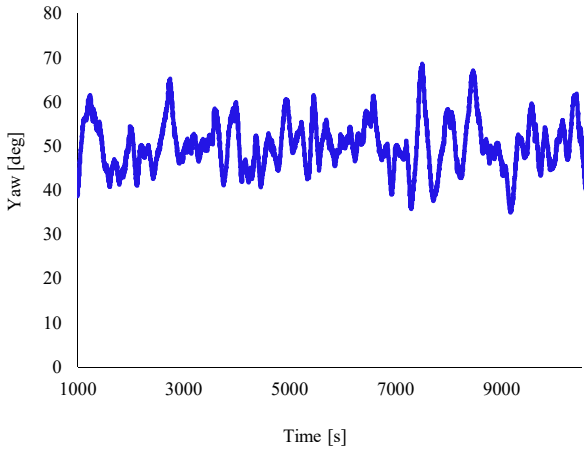

1041

1042 **Fig. 40.** Yaw motion response of the FPSO with mooring lines,

1043 non-collinear case Full Load condition

1044

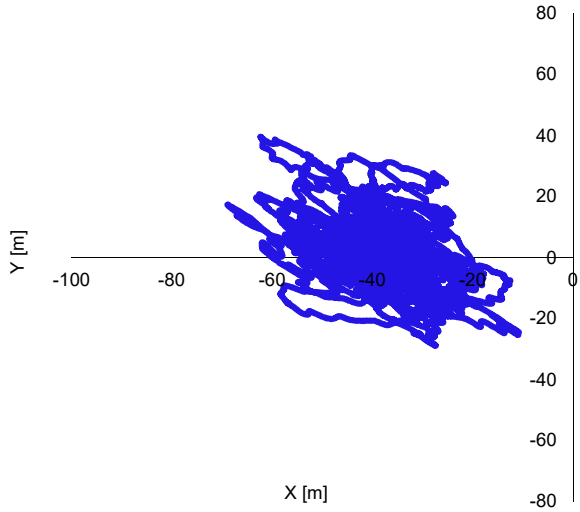

1045

1046 **Fig. 41.** Offsets trajectories of the FPSO with mooring lines, non-

1047 collinear case Ballast Load condition

1048

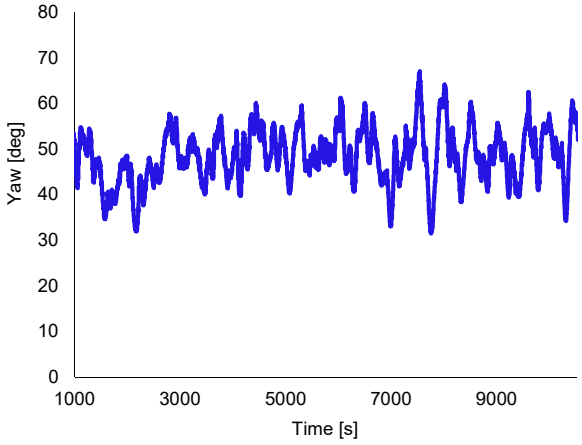

1049

1050 **Fig. 42.** Yaw motion response of the FPSO with mooring lines,

1051 non-collinear case Ballast Load condition

1052

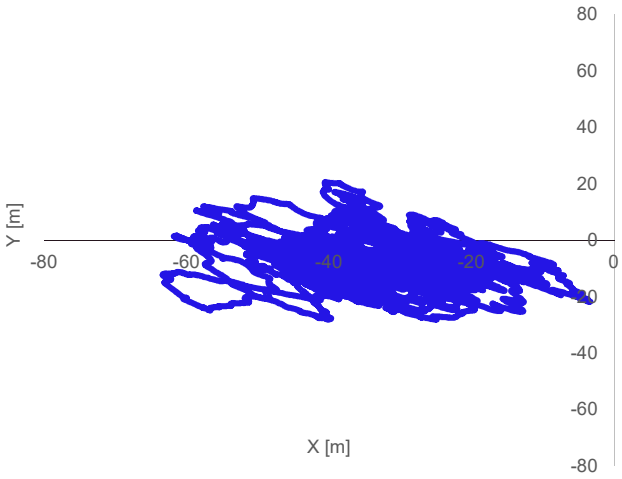

Fig. 43. Offsets trajectories of the FPSO with mooring lines and risers, non-collinear case Ballast Load condition

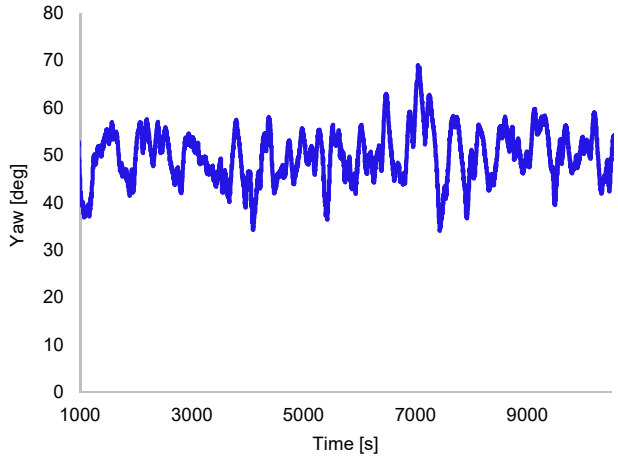

Fig. 44. Yaw motion response of the FPSO with mooring lines and risers, non-collinear case Ballast Load condition

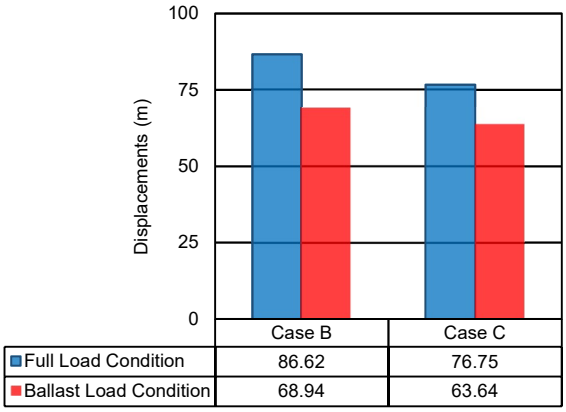

1064

1065 **Fig. 45.** Comparison of the extreme surge motion non-collinear case, FPSO mooring lines (Case B) vs. FPSO

1066 mooring lines and riser (Case C) for the Full load and Ballast load conditions (in terms of absolute values)

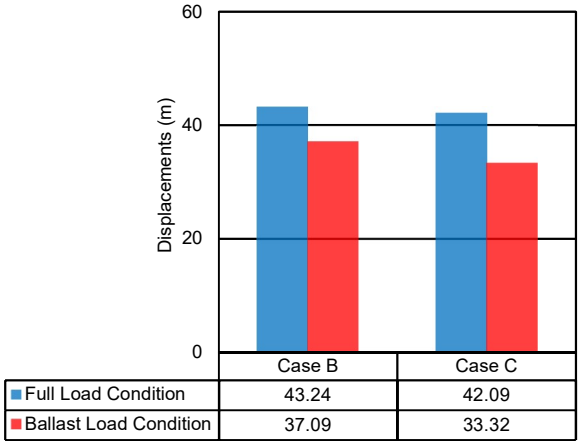

1067

1068 **Fig. 46.** Comparison of the mean surge motion non-collinear case FPSO mooring lines (Case B) vs. FPSO

1069 mooring lines and riser (Case C) for the Full load and Ballast load conditions (in terms of absolute values)

1070

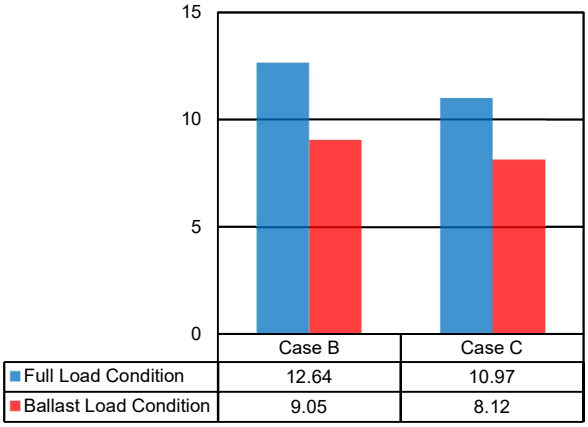

1071

1072 **Fig. 47.** Comparison of the standard deviation of surge motion non-collinear case FPSO mooring lines (Case B)

1073 vs. FPSO mooring lines and riser (Case C) for the Full load and Ballast load condition

1074

1075

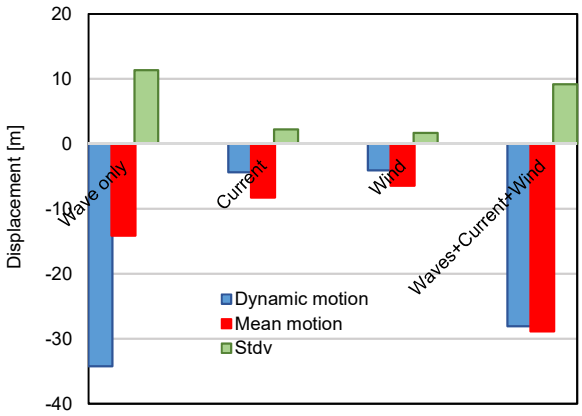

1076

1077 **Fig. 48.** Statistical values of surge motion responses for the Collinear 'In-line' cases for the FPSO with mooring

1078 lines exposed to irregular waves only and irregular waves, current and wind.

1079

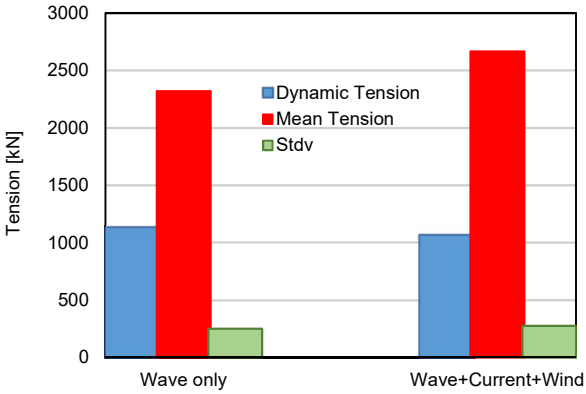

Fig. 49. Statistical values of tension response of the loaded line (L-1) for the Collinear 'In-line' cases for the FPSO with mooring lines exposed to irregular waves only and irregular waves, current and wind.

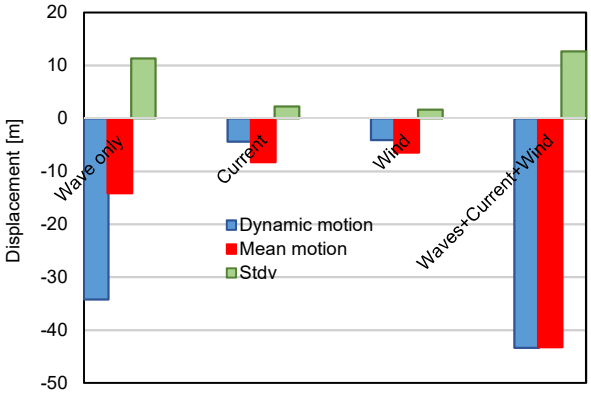

1085

1086 **Fig. 50.** Statistical values of surge motion responses for the Collinear 'In-line' case exposed to irregular waves

1087 only and Non-Collinear cases exposed to irregular waves, current and wind, FPSO model with mooring lines

1088

1089

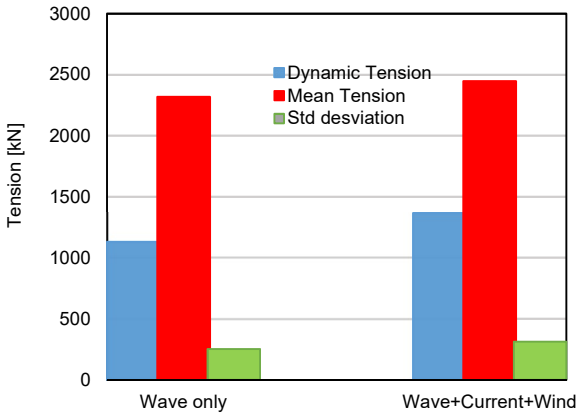

1090

1091 **Fig. 51.** Statistical values of tension response of the loaded line (L-1) for the Collinear 'In-line' and Non-collinear

1092 cases for the FPSO with mooring lines exposed to irregular waves only and irregular waves, current and wind.

1093